FP7-ICT-2011.8
Contract no.: 318493

www.toposys.org

Deliverable D1.1

Progress and Activity Report on WP1

Deliverable Nature:	Report (R)
Dissemination Level: (Confidentiality)	Public (PU)
Contractual Delivery Date:	M12
Actual Delivery Date:	M12
Version:	1.0

Contents

1 Summary

The idea of functoriality is that the relationships between objects are just as important as the objects themselves. In mathematical terms, we must study not only the underlying spaces, which may be finite point clouds, collaboration/social graphs, or configurations of physical objects in space, but we must also study how these change over time in dynamic settings or how different instances relate to each other.

The goals of this work package capture different aspects of this idea, which reflect the different tasks.

1. Persistence of a self map - in the classical case of linear dynamical systems, the space of endomorphisms, that is maps from a space to itself is characterized by its Jordan form. We extend this idea to sampled self maps. By fixing an eigenvalue, we can obtain persistence results on the behaviour of the self map, specifically by looking at the persistence of the corresponding eigenspaces.

2. Cohomology of recurrent systems - recurrence in a configuration space is characterized by a circle. Multiple modes of recurrence are capured by a wedge of circles. We present two methods for utilizing this.
   One is a computational take on a classical approach in dynamical systems, that is on computing the Conley index of a Poincaré map. The Poincaré section can be thought of as a slice though which all periodic orbits of a system must pass through. The Poincaré map is the map of a neighborhood around a point onto the section.
   The second looks at how to capture and reconstruct the modes of recurrence through finding circles in sampled data(including time series data) and automatically parameterizing the modes using persistent cohomology. In principle, this allows us to perform a type of Fourier analysis in more general settings such as metric spaces.

3. Hierarchies of maps - finally we look to examine more general diagrams of vector spaces (or more generally persistence modules). Although a simple barcode or diagram is unlikely to exist, we present a lattice theoretic construction which will ultimately help compare diagrams of different shapes as well as allowing us to perform some analysis on these type of structures, with future work hopefully leading to some form of decomposition.

The final task looks to unify the above approaches, however, it begins in the second year of the project and so is not discussed further.

This report is based on several papers - the section on persistence of a self map is based on

- H. Edelsbrunner, G. Jablonski and M. Mrozek. "The persistent homology of a self-map." Found. Comput. Math., submitted. (attached) - note that the categorical basis for the construction is reported in WP3

The section on cohomology of recurrent systems is based on two papers:

- M. Mrozek, R. Srzednicki, F. Weilandt, "A topological approach to the algorithmic computation of the Conley index of Poincare operators", preprint (attached)

- V. de Silva, P. Skraba and M. Vejdemo-Johansson, "Topological Analysis of Recurrent Systems," Workshop on Algebraic Topology and Machine Learning, NIPS 2012(available at `http://www.cs.cmu.edu/~sbalakri/Topology_final_versions/dS-S-VJ-final.pdf`)

Finally, the initial work on hierarchies of maps, where we complete a diagram of vector spaces into a distrbutive lattice is based upon

- P. Skraba and J. Pita Costa, "On a lattice for persistence," (available at `http://arxiv.org/abs/1307.4192`)

2 Persistence of a self map

Here we look at how to study the persistence of endomorphisms induced in homology by continuous self-maps. The long term goal is to embed persistence in the computational analysis of dynamical systems, as pursued in [13] and the related literature.

In the case of finitely generated homology with field coefficients, the homomorphism induced by a continuous map between topological spaces is a linear map between finite-dimensional vector spaces. Such a map $\varphi : Y \to X$ is characterized up to conjugacy by its rank. This is in contrast to a linear self-map, $\phi : X \to X$, which in the case of an algebraically closed field[1] is characterized up to conjugacy by its Jordan form. A weaker piece of information are the eigenvectors, which in our setting capture the homology classes that are invariant under the self-map. Therefore, it is natural to study the persistence of eigenvalues and eigenspaces as a first step to the full understanding of the persistence of the map. Beyond describing the algorithm for the persistence of eigenvalues and eigenspaces, we analyze its performance, proving that the persistence diagram it produces is stable under perturbations of the input, and the algorithm converges to the homology of the studied map, reaching the correct ranks for a sufficiently fine sample. In addition, we exhibit some preliminary results.

We motivate the technical work in this paper with a small toy example, designed to highlight one of the main difficulties we encounter. Writing $\mathbb{S}^1$ for the circle in the complex plane, we consider the map defined by $f(z) := z^2$, which doubles the angle of the input point. Sampling $\mathbb{S}^1$ at eight equally spaced locations, $x_j := \cos\frac{j\pi}{4} + \mathbf{i}\sin\frac{j\pi}{4}$, we can check that $f(x_j) = x_{2j}$, where indices are taken modulo 8. Assuming the space and the map are unknown, other than at the sampled points and their images, we consider the filtration $K_1 \subseteq K_2 \subseteq K_3 \subseteq K_4 \subseteq K_5$ shown in the top row of Figure 1. Each complex K_i consists of all simplices spanned by the eight points whose diameters do not exceed a given threshold, and this threshold increases from left to right. The most persistent homology classes in this filtration are the component that appears in K_1 and lasts to K_5 and the loop that appears in K_2 and lasts to K_4. We would hope that f extends to simplicial maps on these complexes, but this is unfortunately not the case in general. For instance, f maps the endpoints of the edge x_1x_7 in K_3 to the points x_2 and x_6, but they are not endpoints of a common edge in K_3. The reason for this situation is the expanding character of f. To still make sense of the map, we construct the maximal partial simplicial maps, $\kappa_i : K_i \nrightarrow K_i$ consistent with f. Figure 1 shows the domains of these maps in the bottom row, and for $i = 3, 4$, we can see how κ_i wraps the convex octagon twice around the hole in K_i shown right above. This reflects the fundamental feature of f, namely that its image wraps around the circle twice. To see this more formally, we compare the homology classes in the domains with their images. For $i = 1, 3, 5$ the inclusion of the domain of κ_i in K_i induces an isomorphism in homology. The comparison therefore reduces to the study of eigenvectors of an endomorphism. The lack of isomorphism for $i = 2, 4$ may be overcome by the study of eigenvectors of pairs of linear maps. In this particular case, we are able to conclude that

[1] A field is *algebraically closed* if every non-constant polynomial over the field has a root.

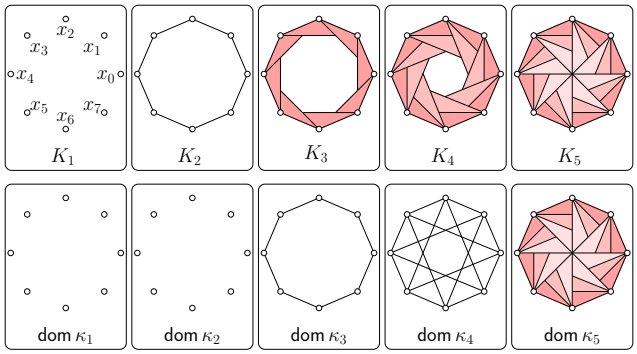

Figure 1: Five simplicial complexes in the filtration of the eight data points at the top, and the domains of the induced partial simplicial maps at the bottom.

the eigenspace for eigenvalue $t = 2$ appears in K_3 and lasts to K_4, thus reconstructing the essential character of f from a very small sample.

To summarize, there are differences between the partial simplicial maps and the underlying continuous map; see in particular the reorganization that takes place at $i = 2$ and $i = 4$. The hope to recover the properties of the latter from the former is based on the ability of persistence to provide a measure that transcends fluctuations and identifies what stays the same when things change.

Partial functions. We recall that a *category* consists of *objects* and (directed) *arrows* between objects. Importantly, there is the *identity arrow* from every object to itself, and arrows compose associatively. An arrow, $\theta : K \to L$, is *invertible* if it has an inverse, $\theta^{-1} : L \to K$, such that $\theta^{-1}\theta$ and $\theta\theta^{-1}$ are the identity arrows for K and L. If there is an invertible arrow from K to L, then the two objects are *isomorphic*. Every category in this paper contains a *zero object*, which is characterized by having exactly one arrow to and one arrow from every other object. It is unique up to isomorphisms. Two arrows, $\kappa : K \to K'$ and $\lambda : L \to L'$ are *conjugate* if there are invertible arrows $\theta : K \to L$ and $\theta' : K' \to L'$ that commute with κ and λ; that is: $\theta'\kappa = \lambda\theta$. A *functor* is an arrow between categories, assigning to each object and each arrow of the first category an object and an arrow of the second category in such a way that the identity arrows are mapped to identity arrows and the functor commutes with the composition of the arrows.

We use a category whose arrows generalize functions between sets as the basis of other categories. Specifically, a *partial function* is a relation $\xi \subseteq X \times Y$ such that every $x \in X$ is either not paired or paired with exactly one element in Y [14]. We denote it by $\xi : X \nrightarrow Y$, observing that there is a largest subset $X' \subseteq X$ such that the restriction $\xi : X' \to Y$ is a function. We call $\mathsf{dom}\,\xi := X'$ the *domain* and $\mathsf{ker}\,\xi := X - X'$ the *kernel* of ξ. For each $x \in X'$, we write $\xi(x)$ for the unique element $y \in Y$ paired with x, as usual. Similarly, we write $\xi(A)$ for the set of elements $\xi(x)$ with $x \in A \cap X'$. The *image* of ξ is of course the entire reachable set, $\mathsf{im}\,\xi := \xi(X)$. If $\xi : X \nrightarrow Y$ and $\eta : Y \nrightarrow Z$ are partial functions, then their *composition* is the partial function $\eta\xi : X \nrightarrow Z$ consisting of all pairs $(x, z) \in X \times Z$ for which there exists $y \in Y$ such that $y = \xi(x)$ and $z = \eta(y)$. Thus, we have a category of sets and partial functions, which we denote as **Part**. The zero object in this category is the empty set, which is connected to all other sets by empty partial functions. It will

be convenient to limit the objects in this category to finite sets.

Matchings. We call an injective partial function $\alpha : A \rightarrowtail B$ a *matching*. Its restriction to the domain and the image is a bijection, hence the name. Bijections have inverses and so do matchings, namely $\alpha^{-1} : B \rightarrowtail A$ with $(b, a) \in \alpha^{-1}$ iff $(a, b) \in \alpha$.[2] Clearly, the composition of two matchings is again a matching. We therefore have a category, and we write **Mch** for this subcategory of **Part**: its objects are finite sets and its arrows are matchings. Writing $[k] := \{1, 2, \ldots, k\}$, we may assume that $A = [p]$ and $B = [q]$, in which p and q are the cardinalities of A and B. Representing the matching by its matrix, $M = (M_{ij})$, we thus get

$$M_{ij} \quad = \quad \begin{cases} 1 & \text{if } (j, i) \in \alpha, \\ 0 & \text{otherwise,} \end{cases}$$

for $j \in [p]$ and $i \in [q]$. Matrices of matchings are characterized by having at most one non-zero entry in each row and in each column. It follows that there are equally many non-zero rows (the cardinality of the image) as there are non-zero columns (the cardinality of the domain). The *rank* of the matching is this common cardinality, $\mathsf{rank}\,\alpha := \#\mathsf{dom}\,\alpha = \#\mathsf{im}\,\alpha$. The simple structure of matchings makes it easy to compute the ranks of compositions. Letting $\beta : B \rightarrowtail C$ be another matching, the rank of $\beta\alpha : A \rightarrowtail C$ is the cardinality of $\mathsf{im}\,\alpha \cap \mathsf{dom}\,\beta$; see Figure 2. We can rewrite

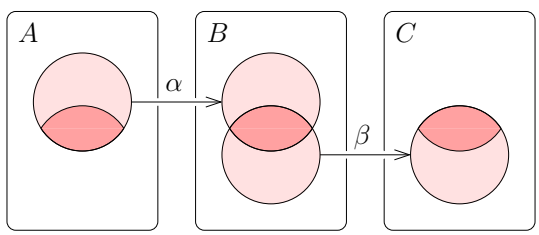

Figure 2: The composition of two matchings. Its domain and image are the dark regions in A and in C.

this as

$$\#(\mathsf{dom}\,\beta - \mathsf{im}\,\alpha) \quad = \quad \mathsf{rank}\,\beta - \mathsf{rank}\,\beta\alpha. \tag{1}$$

It will be useful to extend this relation to the composition of three matchings, adding $\gamma : C \rightarrowtail D$ to the two we already have. The number of elements in the domain of β that are neither in the image of α nor map to the domain of γ is

$$\begin{aligned} \#(\mathsf{dom}\,\beta - \mathsf{im}\,\alpha - \mathsf{dom}\,\gamma\beta) \quad &= \\ \mathsf{rank}\,\beta - \mathsf{rank}\,\beta\alpha - \mathsf{rank}\,\gamma\beta + \mathsf{rank}\,\gamma\beta\alpha. \end{aligned} \tag{2}$$

To see the second line, we construct a set Ω, first by taking the disjoint union of the sets A, B, C, D, and second by identifying two elements if they occur in a common pair, which may be in α, β, or

[2] To be more precise, we should call it a *weak inverse*, because $\alpha^{-1}\alpha$ and $\alpha\alpha^{-1}$ are identities on the domain and image of α and not necessarily on A and B. We simplify language by ignoring this subtlety.

γ. After identification, each matching is a subset of Ω, namely $\alpha = A \cap B$, $\beta\alpha = A \cap B \cap C$, etc. Using the identification, the left-hand side of (2) may be rewritten as the cardinality of the set

$$\begin{aligned}(B \cap C) - (A \cap B) - (B \cap C \cap D) \quad &= \\ (B \cap C) - [(A \cap B \cap C) \cup (B \cap C \cap D)]. \quad &\end{aligned} \tag{3}$$

By elementary inclusion-exclusion, its cardinality is the right-hand side of (2).

Linear maps. Assuming a fixed field, we now consider the category **Vect**, whose objects are the finite-dimensional vector spaces over this field, and whose arrows are the linear maps between these vector spaces. The *dimension* of a vector space, U, is of course the cardinality of its basis, which we denote as $\dim U$. Letting $\upsilon : U \to V$ be a linear map, we write $\mathsf{ker}\,\upsilon := \upsilon^{-1}(0)$ for the *kernel*, $\mathsf{im}\,\upsilon := \upsilon(U)$ for the *image*, and $\mathsf{rank}\,\upsilon := \dim \upsilon(U)$ for the *rank* of υ. Given bases A of U and B of V, we construct the matrix $M = (M_{ij})$ of υ in these bases. In particular, M_{ij} is the coefficient of the i-th basis vector of B in the representation of the image of the j-th basis vector of A. It is generally not the matrix of a matching because υ does generally not map A to B. However, if M is the matrix of a matching, then the partial function $\alpha : A \nrightarrow B$, consisting of all pairs $(a, b) \in A \times B$ with $\upsilon(a) = b$, is a matching that satisfies $\mathsf{ker}\,\alpha = \mathsf{ker}\,\upsilon \cap A$, $\mathsf{im}\,\alpha = \mathsf{im}\,\upsilon \cap B$, and, most importantly,

$$\mathsf{rank}\,\alpha \quad = \quad \mathsf{rank}\,\upsilon. \tag{4}$$

A matching with this property exists, and we can compute it by reducing M to Smith normal form. However, it is not necessarily unique. On the other hand, any two matchings $\alpha : A \nrightarrow B$ and $\alpha' : A' \nrightarrow B'$ that satisfy (4) – albeit possibly for different bases A, A' of U and B, B' of V – are conjugate in **Mch**. Indeed, we have $\#A = \#A'$, $\#B = \#B'$, and $\mathsf{rank}\,\alpha = \mathsf{rank}\,\alpha'$ from (4), which suffices for the existence of bijections that imply the conjugacy of α and α'.

Eigenvalues and eigenspaces. Still assuming the same field, we consider a vector space, U, and a linear self-map, $\phi : U \to U$. Letting t be an element in the field, we set

$$E_t(\phi) \quad := \quad \{u \in U \mid \phi(u) = tu\}. \tag{5}$$

If $E_t(\phi) \neq 0$, then t is an *eigenvalue* of ϕ, and $E_t(\phi)$ is the corresponding *eigenspace*. As usual, the non-zero elements of $E_t(\phi)$ are referred to as the *eigenvectors* of ϕ and t. It should be clear that $E_t(\phi)$ is a subspace of U and thus a vector space itself. We find it convenient to formalize the transition from the linear self-map to its eigenspaces. To this end, we consider another endomorphism, $\phi' : U' \to U'$, and a linear map $\upsilon : U \to U'$ such that

$$\begin{array}{ccc} U & \xrightarrow{\phi} & U \\ \downarrow{\scriptstyle \upsilon} & & \downarrow{\scriptstyle \upsilon} \\ U' & \xrightarrow{\phi'} & U' \end{array} \tag{6}$$

commutes. We can think of this diagram as an arrow in a new category **Endo**(**Vect**); see e.g. [18]. In particular, the objects in **Endo**(**Vect**) are the endomorphisms in **Vect**, and the arrows are the linear maps that commute with the endomorphisms. Fixing t, we now map ϕ to $E_t(\phi)$ and ϕ' to $E_t(\phi')$, which are objects in **Vect**. Since (6) commutes, the image of an eigenvector in $E_t(\phi)$ belongs to $E_t(\phi')$. This motivates us to define the restriction of υ to $E_t(\phi)$ and $E_t(\phi')$ as the image of υ under E_t, thus completing the definition of E_t as the *eigenspace functor* from **Endo**(**Vect**) to **Vect**.

Eigenspace functor for pairs. The situation in this paper is more general, and we need an extension from endomorphisms to pairs of linear maps. Let $\varphi, \psi : U \to V$ be such a pair, and define $\bar{E}_t(\varphi, \psi) := \{u \in U \mid \varphi(u) = t\psi(u)\}$. This is a subspace of U, but it contains the entire intersection of the two kernels, which we remove by taking the quotient:

$$E_t(\varphi, \psi) \quad := \quad \bar{E}_t(\varphi, \psi) / \left(\ker \varphi \cap \ker \psi\right). \tag{7}$$

Assuming $E_t(\varphi, \psi) \neq 0$, we call t an *eigenvalue* of the pair, and $E_t(\varphi, \psi)$ the corresponding *eigenspace*. The non-zero elements of $E_t(\varphi, \psi)$ are the *eigenvectors* of φ, ψ, and t. Similar to the case of endomorphisms, $E_t(\varphi, \psi)$ is a vector space, although its elements are not the original vectors but equivalence classes of such. To formalize the transition, we consider a second pair $\varphi', \psi' : U' \to V'$ and linear maps υ and ν such that

$$\begin{tikzcd} V \arrow[d, "\nu"] & U \arrow[l, "\varphi"'] \arrow[r, "\psi"] \arrow[d, "\upsilon"] & V \arrow[d, "\nu"] \\ V' & U' \arrow[l, "\varphi'"'] \arrow[r, "\psi'"] & V' \end{tikzcd} \tag{8}$$

commutes. We can think of this diagram as an arrow in a new category as follows. The objects in **Pairs**(**Vect**) are the horizontal pairs of linear maps, and the arrows are the vertical pairs of linear maps that form commutative diagrams, as in (8). Fixing t, we can now map φ, ψ to $E_t(\varphi, \psi)$ and φ', ψ' to $E_t(\varphi', \psi')$, which are objects in **Vect**. Since (8) commutes, the images of the vectors in a class $[u] \in E_t(\varphi, \psi)$ form an equivalence class $[\upsilon(u)] \in E_t(\varphi', \psi')$. We thus define the arrow that maps $[u]$ to $[\upsilon(u)]$ as the image of υ, ν under E_t. This completes the definition of E_t as the *eigenspace functor* from **Pairs**(**Vect**) to **Vect**.

It is easy to see that if the vertical maps in (8) are isomorphisms, then $E_t(\varphi, \psi)$ and $E_t(\varphi', \psi')$ are isomorphic. Starting with (8), suppose now that $V = V' = U'$ and that ν and φ' are identities, and redraw the diagram in triangular form:

$$\begin{tikzcd} & U \arrow[dl, "\varphi"'] \arrow[dr, "\psi"] & \\ V \arrow[rr, "\psi'"] & & V \end{tikzcd} \quad . \tag{9}$$

If φ is an isomorphism, then so is υ, which implies that $E_t(\varphi, \psi)$ and $E_t(\psi')$ are isomorphic. This little fact will be useful in Section 2.2, when we analyze our algorithm by comparing eigenspaces obtained from endomorphisms and from pairs of linear maps.

2.1 Algorithm

Assuming a hierarchical representation of an endomorphism, we explain how to compute the persistent homology of its eigenspaces in three steps. The general setting consists of a filtration and an increasing sequence of self-maps. In Step 1, we compute the bases of the two towers obtained by applying the homology functor to the filtrations of spaces and domains. In Step 2, we construct matrix representations of the linear maps in the morphism between the two towers. In Step 3, we compute the eigenvalues and the corresponding eigenspaces as well as their persistence.

Hierarchical representation. The algorithm does its computations on a simplicial complex, K, and a partial simplicial map, $\kappa : K \rightarrowtail K$. More precisely, κ is a partial map on the underlying space of K, but we will ignore this difference. In addition, we assume a filtration of the complex, $\emptyset = K_0 \subseteq K_1 \subseteq \ldots \subseteq K_n = K$, and of the domain,

$$\mathsf{dom}\,\kappa_0 \;\subseteq\; \mathsf{dom}\,\kappa_1 \;\subseteq\; \ldots \;\subseteq\; \mathsf{dom}\,\kappa_n, \tag{10}$$

with $\kappa_i : K_i \rightarrowtail K_i$ being the two-sided restriction of κ to K_i. Writing **Simp** for the category of simplicial complexes and simplicial maps, we use the two filtrations to form a tower in **Pairs**(**Simp**). Its objects are the pairs $\iota_i, \kappa'_i : \mathsf{dom}\,\kappa_i \to K_i$, in which ι_i is the inclusion and κ'_i is the further restriction of κ_i to the domain. Its arrows are the commuting diagrams connecting contiguous objects by inclusions. Applying the homology functor, we get a tower in **Pairs**(**Vect**), and applying the eigenspace functor, we get a tower in **Vect**. The algorithm in this section computes the persistence diagram of the latter tower.

In principle, it is irrelevant how K and κ are obtained. In the context of sampling an unknown map, we may construct both from a finite sample of that map. We explain this in detail. Write $\mathrm{Vert}\,K$ for the vertex set of K, and let $g : \mathrm{Vert}\,K \rightarrowtail \mathrm{Vert}\,K$ be a partial function from the vertex set to itself. If the vertices of a simplex $\sigma \in K$ map to the vertices of a simplex $\tau \in K$, then we extend the vertex map linearly to σ as follows. Letting $x_0, x_1, \ldots, x_p$ be the vertices, and $x = \sum_{i=0}^{p} \lambda_i x_i$ a point of σ, where $\sum_{i=0}^{p} \lambda_i = 1$ and $\lambda_i \geqslant 0$ for all i, we define

$$\kappa(x) \quad := \quad \sum_{i=0}^{p} \lambda_i g(x_i), \tag{11}$$

which is a point of τ. Doing this for all such simplices σ, we get a partial simplicial map, $\kappa : K \rightarrowtail K$. Its domain consists of all simplices whose vertices map to the vertices of a simplex in K. Having constructed κ, it is now easy to construct the partial simplicial maps on the subcomplexes of K. Letting $g_i : \mathrm{Vert}\,K_i \rightarrowtail \mathrm{Vert}\,K_i$ be the restriction of g to the vertex set of K_i, we get $\kappa_i : K_i \rightarrowtail K_i$ by linear extension as before; it is also the restriction of κ to K_i, as mentioned earlier. We observe that the image is not necessarily the same as the domain. This difference is the reason we construct the tower in **Pairs**(**Simp**) and not in **Endo**(**Simp**), as explained above. Finally, we note that the domains of the κ_i form the filtration (10), as required. Indeed, if the vertices of a simplex σ in K_i map to the vertices of a simplex τ in K_i, then $\sigma \in \mathsf{dom}\,\kappa_j$ for all $i \leqslant j \leqslant n$.

Assuming the above hierarchical representation of the sampled map, we explain now how to compute the persistent homology of its eigenspaces in three steps. In Step 1, we compute the bases of the two towers obtained by applying the homology functor to the filtrations of spaces and domains. In Step 2, we construct matrix representations of the linear maps in the morphism between the two towers. In Step 3, we compute the eigenvalues and the corresponding eigenspaces as well as their persistence.

Step 1: spaces. Applying the homology functor, we get the tower $\mathcal{X} = (X_i, \xi_i)$ from the filtration of domains $\mathsf{dom}\,\kappa_i$, and the tower $\mathcal{Y} = (Y_i, \eta_i)$ from the filtration of complexes K_i. In this step, we compute the bases of these towers, which we explain for $\mathcal{X}$. Importantly, we represent all domains and maps in a single data structure, and we compute the basis in a single step that considers all maps at once.

Call $\mathsf{dom}\,\kappa_i - \mathsf{dom}\,\kappa_{i-1}$ the *i-th block* of simplices, and sort $\mathsf{dom}\,\kappa$ as $\sigma_1, \sigma_2, \ldots, \sigma_m$ such that each simplex succeeds its faces, and the i-th block succeeds the $(i-1)$-st block, for every $1 \leqslant i \leqslant n$.

Let D be the ordered boundary matrix of $\mathsf{dom}\,\kappa$; that is: $D[k,\ell]$ is non-zero if σ_k is a codimension-1 face of σ_ℓ, and $D[k,\ell] = 0$, otherwise. The ordering implies that the submatrix consisting of the first i blocks of rows and the first i blocks of columns is the boundary matrix of $\mathsf{dom}\,\kappa_i$, for each i. We use the original persistence algorithm [9, Chapter VII.1] to construct the basis. Similar to the echelon form, it creates a collection of distinguished non-zero entries, at most one per column and row, but to preserve the order, it does not arrange them in a staircase. Specifically, the algorithm uses left-to-right column additions to get D into *reduced form*, which is a matrix R so that the lowest non-zero entries of the columns belong to distinct rows. Suppose $R[k,\ell+1]$ is the lowest

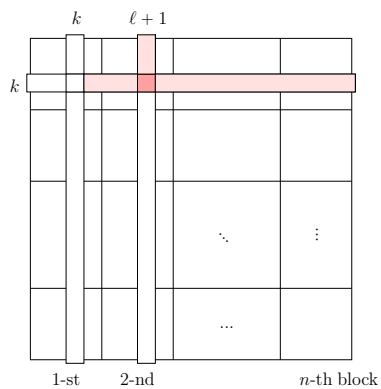

Figure 3: The rows and columns of the reduced matrix are decomposed into n blocks each. The k-th column is zero, and the lowest non-zero entry in the $(\ell+1)$-st column belongs to the k-th row. Since the k-th and $(\ell+1)$-st columns belong to the first and the second blocks, the corresponding persistence interval is $[1,1]$.

non-zero entry in column $\ell+1$, as in Figure 3. Then $R[.,k] = 0$ and $b_{\ell+1} := R[.,\ell+1]$ is the boundary of a chain that contains $\sigma_{\ell+1}$. We note that $b_{\ell+1}$ existed as early as X_k but not earlier, and that it changed to a boundary in $X_{\ell+1}$ but not earlier. In other words, $b_{\ell+1} \notin \mathsf{im}\,\xi_{k-1}$ and $b_{\ell+1} \in \mathsf{ker}\,\xi_\ell$, as required for a maximal interval. Assuming σ_k belongs to the i-th block of simplices, and $\sigma_{\ell+1}$ belongs to the $(j+1)$-st block, the corresponding persistence interval is $[i,j]$. It is empty if $i = j+1$. In the persistence literature, the above situation is expressed by saying that b_ℓ is *born* at X_i and *dies entering* X_{j+1}. It is also possible that a cycle is born but never dies, in which case we do not have a corresponding lowest non-zero entry in the matrix. But this case can easily be avoided, for example by adding the cone over the entire complex as a last block of simplices to the filtration.

Given an index $1 \leqslant i \leqslant n$, we identify the persistence intervals that contain i and get a basis of X_i by gathering the vectors in the corresponding columns of R. The collection of these bases form a basis of $\mathcal{X}$.

Running the same algorithm on the filtration of K, we get a basis of $\mathcal{Y}$.

Step 2: maps. Let $\varphi, \psi_i : \mathcal{X} \to \mathcal{Y}$ be the morphisms such that φ_i is induced by $\iota_i : \mathsf{dom}\,\kappa_i \to K_i$ and ψ_i is induced by $\kappa'_i : \mathsf{dom}\,\kappa_i \to K_i$. In the second step of the algorithm, we construct matrix representations of the two morphisms. Both matrices, Φ for φ and Ψ for ψ, have their columns indexed by the non-zero columns of the reduced matrix of $\mathcal{X}$ and their rows indexed by the non-zero

columns of the reduced matrix of $\mathcal{Y}$. We explain the computations for Ψ.

Letting $R[.,\ell+1]$ be a non-zero column in the reduced matrix of $\mathcal{X}$, we recall that $b_{\ell+1} = R[.,\ell+1]$ is a cycle in $\mathsf{dom}\,\kappa$. First, we compute its image, $c_{\ell+1} := \kappa(b_{\ell+1})$, which either collapses to zero or is a cycle of the same dimension in $\mathsf{im}\,\kappa$. Second, we write the homology class of $c_{\ell+1}$ as a linear combination of the basis vectors of Y_j, assuming σ_ℓ belongs to the j-th block of simplices, as before. Most effectively, this is done as part of the reduction of the boundary matrix of K. Indeed, we can insert the images of the columns into the boundary matrix so that their representation as linear combinations of basis vectors of $\mathcal{Y}$ falls out as a by-product of the reduction. Running the same algorithm for φ, we get the matrix Φ.

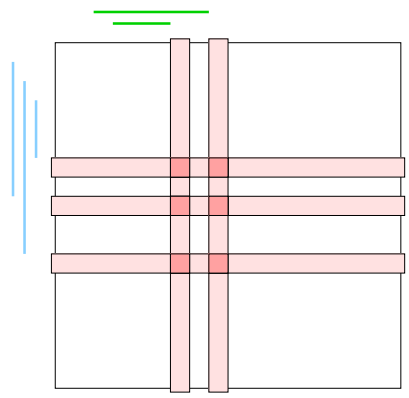

Figure 4: Extracting the matrix representation of ψ_i from Ψ. For each persistence interval that contains i, we show the row or column that stores the corresponding cycle.

The two computed matrices represent the morphisms, φ and ψ, from which the matrices Φ_i and Ψ_i representing the arrows, φ_i and ψ_i, can be extracted. To do so, we first find all persistence intervals that contain i, as before. Second, we collect the intersections of all corresponding rows and columns, as illustrated in Figure 4.

Step 3: eigenspaces. We recall that Step 2 provides presentations of φ and ψ in terms of the same bases, namely those of $\mathcal{X}$ and of $\mathcal{Y}$ as computed in Step 1. In this step, we compute the filtration of eigenspaces and their persistence, separately for each eigenvalue $t \neq 0$. Fixing the eigenvalue, we compute the eigenspaces of φ_i and ψ_i and we take the quotient relative to the intersection of kernels:

$$\bar{E}_t(\varphi_i,\psi_i) = \mathsf{ker}\,(\varphi_i - t\psi_i), \tag{12}$$

$$E_t(\varphi_i,\psi_i) = \bar{E}_t(\varphi_i,\psi_i)/\left(\mathsf{ker}\,\varphi_i \cap \mathsf{ker}\,\psi_i\right). \tag{13}$$

It might be interesting to do the computations incrementally, as in Steps 1 and 2, but here we have to add as well as remove rows and columns, which makes the update operation complicated. Besides, the matrices at this stage tend to be small (see Table 1), so we decide to do the computations for each index i from scratch. At the same time, we extract the kernels of φ_i and ψ_i from Φ_i and Ψ_i, and we use standard methods from linear algebra to compute the quotient. Next, we compute the maps $\xi_i : \mathsf{dom}\,\kappa_i \to \mathsf{dom}\,\kappa_{i+1}$ and their restrictions $\epsilon_{t,i} : E_t(\varphi_i,\psi_i) \to E_t(\varphi_{i+1},\psi_{i+1})$, thus

completing the construction of the eigenspace tower defined by φ and ψ. Finally, we compute the persistence of this tower.

2.2 Analysis

Given a finite set of sample points and their images, we apply the algorithm of Section 2.1 to compute information about the otherwise unknown map acting on an unknown space. In this section, we prove that under mild assumptions – about the space, the map, and the sample – this information includes the correct dimension of the eigenspaces. We also show that the persistence diagrams of the eigenspace towers are stable under perturbations of the input.

Graphs and distances. Let $f : \mathbb{X} \to \mathbb{X}$ be a continuous map acting on a topological space. For convenience, we assume that $\mathbb{X}$ is a subset of $\mathbb{R}^\ell$, with topology induced by the Euclidean metric.[3] While we are interested in exploring f, we assume that all we know about it is a finite set, $S \subseteq \mathbb{X}$, and the image, $f(s)$, for every point $s \in S$. Assuming that the image of every point is again in S, we write $g : S \to S$ for the restriction of f.[4] The goal is to show that under reasonable conditions, f and g are similar so that we can learn about the former by studying the latter. To achieve this, we need some way to measure distance between two functions whose domains need not be the same. To this end, we consider the graphs of the functions,

$$Gf := \{(x, f(x)) \mid x \in \mathbb{X}\}, \tag{14}$$

$$Gg := \{(s, g(s)) \mid s \in S\}, \tag{15}$$

which are both subsets of $\mathbb{R}^\ell \times \mathbb{R}^\ell$. Using the product metric, the distance between (x, x') and (y, y') in the product space is the larger of the two Euclidean distances, $\|x - y\|$ and $\|x' - y'\|$. We compare two maps using the *Hausdorff distance* between their graphs. Recall that the Hausdorff distance between two sets is the infimum radius, r, such that every point of either set has a point at distance at most r in the other set. We note that the Hausdorff distance between the domains of the two functions is bounded from above by the Hausdorff distance between their graphs:

$$\mathrm{Hdf}(\mathbb{X}, S) \leqslant \mathrm{Hdf}(Gf, Gg), \tag{16}$$

simply because the distance between two points in $\mathbb{R}^\ell \times \mathbb{R}^\ell$ is at least the distance between their projections to the first factor. The Hausdorff distance between two sets is related to the difference between the distance functions they define. To explain this, let $d_{\mathbb{X}}, d_S : \mathbb{R}^\ell \to \mathbb{R}$ be the functions that map each point y to the infimum distance to a point in $\mathbb{X}$ and S, respectively. Similarly, let $d_{Gf}, d_{Gg} : \mathbb{R}^\ell \times \mathbb{R}^\ell \to \mathbb{R}$ be the corresponding distance functions in the product space. Then we have

$$\|d_{\mathbb{X}} - d_S\|_\infty = \mathrm{Hdf}(\mathbb{X}, S), \tag{17}$$

$$\|d_{Gf} - d_{Gg}\|_\infty = \mathrm{Hdf}(Gf, Gg). \tag{18}$$

[3] With occasionally more elaborate formalism, everything we say can be generalized to $\mathbb{X}$ embedded in a general metric space.

[4] In cases in which the image of a point is not in S, we can snap the image to the nearest point in S, which usually implies only a small perturbation of the map. Similarly, we can relax the assumption that g be a restriction of f to allow for errors due to noise, for imprecision of measurement, and for approximations in computation.

The conditions under which we can infer properties of f from g include that for small distance thresholds, the sublevel sets of $d_{\mathbb{X}}$ have the same homology as $\mathbb{X}$. To quantify this notion, we assume that $d_{\mathbb{X}}$ is *tame*, by which we mean that every sublevel set has finite-dimensional homology groups, and there are only finitely many *homological critical values* that are the values at which the homology of the sublevel set changes non-isomorphically. Following [5], we define the *homological feature size* of $\mathbb{X}$ as the smallest positive homological critical value of $d_{\mathbb{X}}$, denoting it as $\mathrm{hfs}(\mathbb{X})$. Similarly, we assume that d_{Gf} is tame, and we define $\mathrm{hfs}(Gf)$.

We note that there are functions f for which $\mathrm{hfs}(\mathbb{X}) < \mathrm{hfs}(Gf)$, but there are also functions for which the relation is reversed. For example, the graph of the function that wraps the unit circle in $\mathbb{R}^2$ k times around itself is a curve on a torus in $\mathbb{R}^4$. For large values of k, thickening this curve by a small radius suffices to get the same homotopy type as the torus, while thickening the circle by the same radius does not change its homotopy type.

Sublevel sets. If f and g are similar, then the sublevel sets of their distance functions are similar. To make this more precise, we write $A_r := d_A^{-1}[0, r]$, where A may be $\mathbb{X}$, S, Gf, Gg, or some other set. Then

$$\mathbb{X}_r \subseteq S_{r+\varepsilon} \subseteq \mathbb{X}_{r+2\varepsilon}, \tag{19}$$

$$Gf_r \subseteq Gg_{r+\varepsilon} \subseteq Gf_{r+2\varepsilon}, \tag{20}$$

provided $\varepsilon \geqslant \mathrm{Hdf}(Gf, Gg)$, which we recall is at least the Hausdorff distance between $\mathbb{X}$ and S. This suggests that we compare f and g based on the sublevel sets of the four distance functions, which is the program we follow.

We use an indirect approach that encodes the sublevel sets in computationally more amenable simplicial complexes. To explain this connection, we construct a complex by drawing a ball of radius r around each point of S, and let $K_r = K_r(S)$ be the nerve of this collection. It is sometimes referred to as the *Čech complex* of S and r; see [9, Chapter III]. Similarly, we let $L_r = L_r(Gg)$ be the Čech complex of Gg and r.[5] While the complexes are abstract, they are constructed over geometric points, which we use to form maps. Specifically, we write $p_r : L_r \to K_r$ for the simplicial map we get by projecting $\mathbb{R}^\ell \times \mathbb{R}^\ell$ to the first factor, and we write $q_r : L_r \to K_r$ if we project to the second factor. Both are simplicial maps because for every simplex in L_r, its projections to the two factors both belong to K_r. Note that p_r is injective, which implies that its inverse is a partial simplicial map, $p_r^{-1} : K_r \nrightarrow L_r$, and its restriction to the domain is a simplicial isomorphism. Composing it with q_r, we get the partial simplicial map $q_r p_r^{-1} : K_r \nrightarrow K_r$.

There, we begin with a partial simplicial map, $\kappa : K \nrightarrow K$, and a filtration of K. The filtration is furnished by the sequence of Čech complexes of S, which ends with the complete simplicial complex K over the points in S, and κ is the partial simplicial map defined by $g : S \to S$. In this case, κ happens to be a simplicial map because K is complete. For each radius, r, we have defined $\kappa_r : K_r \nrightarrow K_r$ as the restriction of κ, which is a partial simplicial map. It is not difficult to prove that κ_r is equal to the map we have obtained by composing p_r^{-1} and q_r before. We state this result and its consequence for towers of eigenvalues without proof.

[5] A practically more convenient alternative is the *Vietoris-Rips complex* that consists of all simplices spanned by the data points whose diameters do not exceed $2r$. We will use it for the computations discussed in Section 2.3, but for now we stay with the Čech complex, which has the theoretical advantage that its homotopy type agrees with that of the sublevel set for the same r.

Lemma 2.1 (Projection Lemma)**.** *Let $\kappa_r : K_r \nrightarrow K_r$ be the partial simplicial map obtained by restricting κ to K_r, and let $p_r, q_r : L_r \to K_r$ be the simplicial maps induced by projecting to the two factors. Then $\kappa_r = q_r p_r^{-1}$, for every $r \geqslant 0$.*

Recall that κ'_r is the restriction of κ_r to the domain, and $\iota_r : \mathsf{dom}\,\kappa_r \to K_r$ is the inclusion map. In view of the Projection Lemma, we can freely move between the tower of eigenspaces we get for (ι, κ') and (p, q), which we do in the sequel.

Interleaving. We prepare the main results of this section with a technical lemma about interleaving arrows between eigenspaces. Let $\mathbb{U}, \mathbb{V} \subseteq \mathbb{R}^\ell$, let $h : \mathbb{U} \to \mathbb{U}$ and $k : \mathbb{V} \to \mathbb{V}$ be self-maps, and set $\varepsilon := \mathrm{Hdf}(Gh, Gk)$. Projecting a sublevel set of the distance function of the graph to those of the two factors, we get an object in **Pairs**(**Top**) for h, and another such object for k. Choosing the distance thresholds so they satisfy $r + \varepsilon \leqslant r'$, we have inclusions and therefore an arrow in **Pairs**(**Top**):

$$\begin{tikzcd} \mathbb{U}_r \arrow[d] & Gh_r \arrow[l, "p_r"'] \arrow[r, "q_r"] \arrow[d] & \mathbb{U}_r \arrow[d] \\ \mathbb{V}_{r'} & Gk_{r'} \arrow[l, "p_{r'}"'] \arrow[r, "q_{r'}"] & \mathbb{V}_{r'} \end{tikzcd} . \tag{21}$$

Applying now the homology functor, we get an arrow in **Pairs**(**Vect**), where we write φ_r, ψ_r and $\upsilon_{r'}$, $\nu_{r'}$ for the maps induced in homology. Next applying the eigenspace functor, we get the arrow $E_t(\varphi_r, \psi_r) \to E_t(\upsilon_{r'}, \nu_{r'})$ in **Vect**. The technical lemma states two kinds of interleaving patterns, (22) and (23), with the main difference being the reversed direction on the right.

Lemma 2.2 (Interleaving Lemma)**.** *Let $\mathbb{U}, \mathbb{V} \subseteq \mathbb{R}^\ell$, and $h : \mathbb{U} \to \mathbb{U}$, $k : \mathbb{V} \to \mathbb{V}$ be such that the associated distance functions are tame. Set $\varepsilon := \mathrm{Hdf}(Gh, Gk)$. If $a + \varepsilon \leqslant b \leqslant c \leqslant d - \varepsilon$, then*

$$\begin{tikzcd} E_t(\varphi_a, \psi_a) \arrow[r] \arrow[d] & E_t(\varphi_d, \psi_d) \\ E_t(\upsilon_b, \nu_b) \arrow[r] & E_t(\upsilon_c, \nu_c) \arrow[u] \end{tikzcd} \tag{22}$$

commutes. If $a + \varepsilon \leqslant b \leqslant c$ and $a \leqslant d \leqslant c - \varepsilon$, then the following diagram commutes:

$$\begin{tikzcd} E_t(\varphi_a, \psi_a) \arrow[r] \arrow[d] & E_t(\varphi_d, \psi_d) \arrow[d] \\ E_t(\upsilon_b, \nu_b) \arrow[r] & E_t(\upsilon_c, \nu_c) \end{tikzcd} . \tag{23}$$

Small thickenings. To further prepare our first main result, we recall that the projections from the graph of a continuous map commute with the map itself, a fact best expressed using a commutative diagram:

$$\begin{tikzcd} & Gf, Y \arrow[dl, "p,\mu"'] \arrow[dr, "q,\nu"] & \\ \mathbb{X}, X \arrow[rr, "f,\phi"] & & \mathbb{X}, X \end{tikzcd} . \tag{24}$$

Here, we write Y for the homology group of Gf, $\mu : Y \to X$ for the map induced on homology by $p : Gf \to \mathbb{X}$, etc. The restriction of p to Gf and $\mathbb{X}$ is a homeomorphism. We can therefore apply a result which implies that $E_t(\mu, \nu)$ and $E_t(\phi)$ are isomorphic, for every eigenvalue t. This property persists for small thickenings of $\mathbb{X}$ and Gf assuming the two spaces are compact absolute neighborhood retracts; see [19, p. 290, Thm. 10]. While the name is intimidating, the requirements for a space to be called an absolute neighborhood retract are mild. Since $\mathbb{X}$ and Gf are homeomorphic, the graph is a compact absolute neighborhood retract whenever $\mathbb{X}$ is one. The result about thickening such spaces will be useful in the proof of our first main result, so we state this observation more formally, but without proof.

Lemma 2.3 (ANR Lemma)**.** *Let $\mathbb{X} \subseteq \mathbb{R}^\ell$ be a compact absolute neighborhood retract, let $f : \mathbb{X} \to \mathbb{X}$ be such that the associated distance functions are tame, and let r be positive but smaller than* $\min\{\mathrm{hfs}(\mathbb{X}), \mathrm{hfs}(Gf)\}$*. Writing μ_r, ν_r for the maps induced in homology by the restrictions of p, q to Gf_r and $\mathbb{X}_r$, the eigenspace $E_t(\mu_r, \nu_r)$ is isomorphic to $E_t(\phi)$, for every eigenvalue t.*

Convergence. We are now ready to formulate our first main result. As before, we consider a continuous self-map $f : \mathbb{X} \to \mathbb{X}$, and write $\phi : X \to X$ for the endomorphism induced in homology. Let $S \subseteq \mathbb{X}$ be a finite sample of $\mathbb{X}$, and let $g : S \to S$ another map, perhaps the restriction of f to S. As before, we consider the projections from a thickened version of Gg to the two components. Letting φ_r and ψ_r be the corresponding maps induced in homology, we write

$$\epsilon_{t,r}^{r'} : E_t(\varphi_r, \psi_r) \to E_t(\varphi_{r'}, \psi_{r'}) \tag{25}$$

for the map between the eigenspaces. In a nutshell, our result is a relationship between the dimension of $E_t(\phi)$ and the rank of $\epsilon_{t,r}^{r'}$, for special values of r and r'.

Theorem 2.4 (Inference Theorem)**.** *Let $\mathbb{X} \subseteq \mathbb{R}^\ell$ be a compact absolute neighborhood retract, $S \subseteq \mathbb{X}$, and let $f : \mathbb{X} \to \mathbb{X}$, be a map such that the distance functions for $\mathbb{X}$ and Gf are tame. Then any map $g : S \to S$ satisfies*

$$\dim E_t(\phi) \quad = \quad \mathsf{rank}\, \epsilon_{t,\varepsilon}^{3\varepsilon}, \tag{26}$$

for all $\mathrm{Hdf}(Gf, Gg) < \varepsilon < \frac{1}{4} \min\{\mathrm{hfs}(\mathbb{X}), \mathrm{hfs}(Gf)\}$.

The Inference Theorem may be interpreted as a statement of convergence of our algorithm: if the sampling is fine enough then we are guaranteed to get the dimensions of the eigenspaces as dimensions of persistent homology groups.

Stability. Next, we strengthen the convergence result and prove the stability of the persistence diagrams of the eigenspace towers under perturbations of the input. This is interesting because we may sample the same self-map twice and wonder what we can say about the relationship between the two results. Most of the work that allows us to give a meaningful answer to this question has already been done. To set the stage, we consider two self-maps, $h : \mathbb{U} \to \mathbb{U}$ and $k : \mathbb{V} \to \mathbb{V}$, in which both $\mathbb{U}$ and $\mathbb{V}$ are embedded in $\mathbb{R}^\ell$. As before, we assume that the distance functions, $d_\mathbb{U}$, $d_\mathbb{V}$, d_{Gh}, d_{Gk} are tame. We can now form towers in **Pairs**(**Top**) consisting of projections from the sublevel sets of d_{Gh} and d_{Gk} to the sublevel sets of $d_\mathbb{U}$ and $d_\mathbb{V}$. To formalize the result, we define

the *bottleneck distance* between two persistence diagrams as the maximum distance between pairs in an optimal bijection:

$$\mathrm{Bot}(\mathsf{E},\mathsf{F}) \quad = \quad \inf_{\iota:\mathsf{E}\to\mathsf{F}} \max_{P\in\mathsf{E}} \|P-\iota(P)\|_\infty. \tag{27}$$

Here, $P = [a_\mathrm{b}, a_\mathrm{d})$ is a persistence interval in E, now using the original convention in which a_b and a_d are the birth- and death-values. If $Q = [c_\mathrm{b}, c_\mathrm{d})$ is another persistence interval, then we compute $\|P-Q\|_\infty = \max\{|a_\mathrm{b}-c_\mathrm{b}|, |a_\mathrm{d}-c_\mathrm{d}|\}$, as for points in the plane.[6] Letting $\mathcal{E}_t$ and $\mathcal{F}_t$ be the towers of eigenspaces in **Vect** we get for h and k, we write $\mathrm{Dgm}(\mathcal{E}_t)$ and $\mathrm{Dgm}(\mathcal{F}_t)$ for their persistence diagrams.

Theorem 2.5 (Stability Theorem)**.** *Let $\mathbb{U},\mathbb{V} \subseteq \mathbb{R}^\ell$, and $h : \mathbb{U} \to \mathbb{U}$ $k : \mathbb{V} \to \mathbb{V}$ such that the associated distance functions are tame. Then*

$$\mathrm{Bot}(\mathrm{Dgm}(\mathcal{E}_t), \mathrm{Dgm}(\mathcal{F}_t)) \quad \leqslant \quad \mathrm{Hdf}(Gh, Gk). \tag{28}$$

Proof. According to [3, Thm. 4.9], we only need to verify the ε-strong interleaving of the two towers for ε equal to the Hausdorff distance between Gh and Gk, but this is guaranteed by the Interleaving Lemma.

Letting h and k be finite samples of $f : \mathbb{X} \to \mathbb{X}$, the Stability Theorem implies that the information they convey about the given function cannot be arbitrarily different. Setting $h = f$ and $k = g$, the theorem quantifies the extent to which the persistence diagram for the sampled points can deviate from that of the original self-map.

2.3 Experiments

In this section, we present the results of a small number of computational experiments

All experiments are conducted with an Intel Core2 Quad 2.66GHz processor with 8GB RAM, but using only one core. To convey a feeling for the performance of the software, Table 1 states the time needed to process datasets of size between 40 and 140 points, giving complexes between 10 thousand and 460 thousand simplices. We mention that the running time can be further improved.

#points	skeleton	Step 1	Step 2	Step 3
40	0.14	0.39	0.00	0.04
60	0.67	2.12	0.00	0.15
80	2.21	6.84	0.01	0.39
100	5.18	23.49	0.01	0.86
120	11.13	63.09	0.01	1.50
140	19.53	137.86	0.03	2.18

Table 1: Time in seconds for constructing the 2-skeleton of the Vietoris-Rips complex and executing the steps of our algorithm for one eigenvalue.

In particular, the current implementation is generic, working for any field of coefficients, and the code implementing Step 1 has not yet been optimized. Note the dramatic drop in the running time from Step 1 to Step 2. The reason are the surprisingly small numbers of generators needed in the construction of the matrices Φ and Ψ. In the first set of experiments, we get between 3 and

[6] Following [5], we assume that each persistence diagram contains copies of all empty intervals – points of the form (a, a) – which are used to complete a bijection or decrease the maximum distance.

21 generators for the filtration of $\mathsf{dom}\,\kappa$ and between 5 and 24 generators for the filtration of K. Compare this with the 10,700 to 457,450 simplices in the 2-skeleta of the Vietoris-Rips complex which have to be processed in Step 1. The code for Step 3 takes more time than for Step 2 because it executes computationally demanding procedures in linear algebra.

Expansion. In our first set of computational experiments, we consider the unit circle in the complex plane, and the function $f : \mathbb{S}^1 \to \mathbb{S}^1$ defined by $f(z) := z^2$. It maps each point on the circle to the point with twice the angle. The 1-dimensional homology of the circle has rank 1, with the circle itself being a generator. Under f, the image of this generator is the circle that wraps around $\mathbb{S}^1$ twice. We see that the map expands the space, doubling the angle between any two points. Our main interest is to see whether the methods of this paper can detect this simple fact.

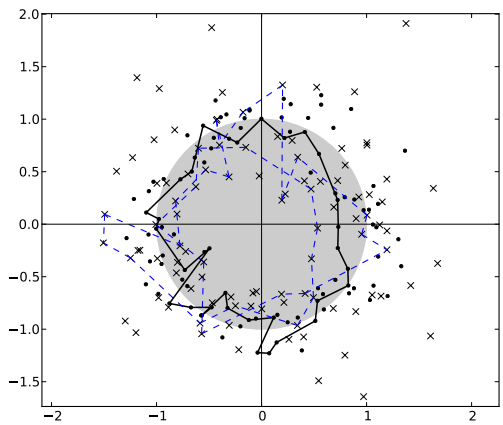

Figure 5: The representation of the function $f(z) := z^2$ using $m = 100$ points with Gaussian noise $\sigma = 0.18$. The dots mark the points in S and the crosses mark their squares. The solid polygon generates the 1-cycle visible in the persistence diagram of the eigenspace tower for eigenvalue $t = 2$; its images is drawn in blue dashed lines and wraps twice around the origin, as expected.

We chose values for three parameters to generate the data sets on which we run our software: the order of the cyclic field, $\mathbb{Z}_k$ with $k = 1009$, the number of points, $m = 100$, and the width of the Gaussian noise, $\sigma \in [0.00, 0.30]$. The finite field is used because we lack a general algorithm for eigenvalues; instead, we try out all possible values. The sample of the function f is computed by picking points $z_j := \cos(\frac{2j\pi}{m}) + \mathbf{i}\sin(\frac{2j\pi}{m})$, for $0 \leqslant i < m$, where $\mathbf{i}$ is the imaginary unit. Next, we let x_j be a point randomly chosen from the isotropic Gaussian kernel with center z_j and width σ. Let S be the set of points x_j. Finally, we set the image of x_j to the point in S that is closest to x_j^2 under the Euclidean metric in the plane. For an example, see Figure 5. The m points define $n \leqslant \binom{m}{2}$ different distances and therefore $n + 1$ different Vietoris-Rips complexes. We are only interested in the 1-dimensional homology, so we can limit ourselves to the 2-skeleta of these complexes. To construct them, we use the algorithm in [21] to compute the complete 2-complex over S. Sorting the edges by length, we get the filtration $K_0 \subseteq K_1 \subseteq \ldots \subseteq K_n$. Figure 6 shows the 1-dimensional persistence diagrams thus obtained for four different values of the width σ. As expected, the persistence of the interval decreases as the noise increases. For $\sigma = 0.30$, we get

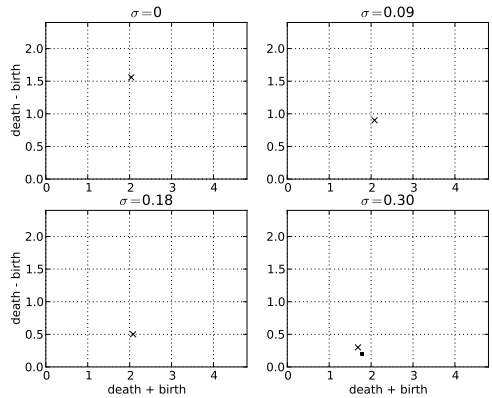

Figure 6: The 1-dimensional persistence diagrams of $f(z) := z^2$ obtained for data that samples the function with Gaussian noise. Crosses mark the persistence intervals for eigenvalue $t = 2$. The dots alert us of the fact that we see this interval for all values, not just for $t = 2$.

a low-persistence interval for every value of t. While we do not observe this all the time, this is a generic phenomenon, and we will shed light on it shortly. For now we just mention that the occurrence of every field value as eigenvalue indicates that we do not have sufficient data to see the features of the map.

Reflection. In our second set of computational experiments, we let $f : \mathbb{S}^1 \to \mathbb{S}^1$ be defined by $f(z) := \bar{z}$, where $\bar{z} = a - \mathbf{i}b$ if $z = a + \mathbf{i}b$. Going around the circle once, in a counterclockwise order, the image under f goes around the circle once in a clockwise order. Again we are interested whether the methods in this paper can detect this fact. The points and their images are chosen in the same way as before, except that the image of x_j is chosen to be the closest point to $\bar{x}_j$. Figure 7 shows the result for $\sigma = 0.27$.

Instead of showing the individual 1-dimensional persistence diagrams, we superimpose them into one diagram. To further facilitate the comparison with the first set of experiments, we draw the superimposed diagrams side by side in Figure 8. In both cases, the Gaussian noise varies between 0.00 and 0.30. We limit the comparison to the eigenvalues $t = 2$ for the expansion and $t = -1$ for the reflection. The diagrams clearly show that the persistence interval shrinks with increasing noise. Indeed, the birth-coordinate grows and the death-coordinate shrinks, so that the sum stays approximately constant, with a faint tendency to shrink. We also see that for the larger noise levels, there are sometimes spurious persistence intervals.

Abundance of eigenvalues. We wish to shed light on the phenomenon that for some datasets and some complexes in the filtration, every field value is an eigenvalue of the pair of linear maps. While it might be surprising at first, there is an elementary explanation that has to do with computing the eigenvalues for a pair instead of a single map.

Here is an illustrative example. Let Y_r be generated by two loops, A and B, and let X_r be generated by a single loop, C. Suppose also that φ_r maps both A and B to C, while ψ_r maps A to C and B to $2C$. Setting $y = iA + jB$, we have $\varphi_r(y) = (i + j)C$ and $\psi_r(y) = (i + 2j)C$. Elementary

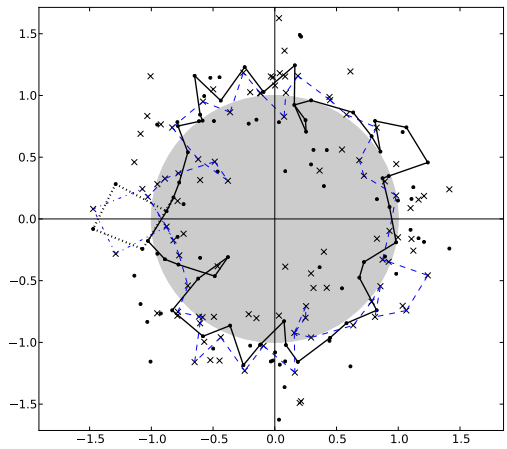

Figure 7: The representation of the function $f(z) := \bar{z}$ using $m = 100$ points with Gaussian noise $\sigma = 0.27$. The solid polygon generates the 1-cycle visible in the persistence diagram of the eigenspace tower for eigenvalue $t = -1$; its image is drawn in blue dashed lines. The dotted polygon generates a second (spurious) 1-cycle in the same diagram. Correspondingly, there are two persistence intervals, drawn as crosses in Figure 8.

number theoretic considerations show that for every $t \in \mathbb{Z}_k$ there are i and j such that $t = \frac{i+j}{i+2j}$. In other words, we can find i and j such that $\varphi_r(y)$ is the t-fold multiple of $\psi_r(y)$. Intersecting the two kernels, we get $i + j = i + 2j = 0$ and therefore $i = j = 0$. Hence, taking the quotient has no effect, implying that $E_t(\varphi_r, \psi_r)$ has non-zero rank for every t. Indeed, because the two loops in Y_r map to different multiples of the same loop in X_r, we have enough flexibility to form combinations whose images under the two maps are arbitrary multiples of each other. This can also happen for an endomorphism $\phi_r : Y_r \to Y_r$, for example by setting $C = B$, but in this case we do not have a second map to compare and therefore get $t = 2$ as the only non-zero eigenvalue.

Let us now look at the linear algebra of the situation. In Step 2, we compute matrices Φ_r and Ψ_r representing $\varphi_r, \psi_r : Y_r \to X_r$, and in Step 3, we compute the null-space of $\Phi_r - t\Psi_r$. The entries of this matrix are degree-1 polynomials in t. Let t_0 be a value at which the matrix reaches its maximum rank, which we denote as k_0. Clearly, $k_0 \leqslant \min\{\#\text{rows}, \#\text{columns}\}$. Note that $\Phi_r - t_0\Psi_r$ has a full-rank minor of size k_0 times k_0. Let $\Delta(t)$ be the determinant of that minor, but now for arbitrary values t. It is a polynomial of degree k_0, and because $\Delta(t_0) \neq 0$, it is not identically zero and therefore has at most k_0 roots. By choice of t_0, this implies that the matrix has maximum rank for all but at most k_0 values of t. Correspondingly, the null-space has minimum dimension, $\#\text{columns} - k_0$, for all but at most k_0 values of t. This is the dimension of $\bar{E}_t(\varphi_r, \psi_r)$. We still take the quotient by dividing with $\ker \varphi_r \cap \ker \psi_r$, which amounts to reducing the dimension by the dimension of that intersection, which we denote as k_1. The resulting dimension of the nullspace is the same for all but at most k_0 values of t, namely $\#\text{columns} - k_0 - k_1$. If $k_1 < \#\text{columns} - k_0$, then $E_t(\varphi_r, \psi_r)$ has positive rank for every value of t. This is what happens for the expanding datasets generated with width $\sigma = 0.15, 0.24, 0.30$ and for the persistence intervals represented by the dots in the left diagram in Figure 8. In all other cases, we have $k_1 = \#\text{columns} - k_0$.

In conclusion, we mention that the extension of the eigenvalue problem to pairs of linear maps

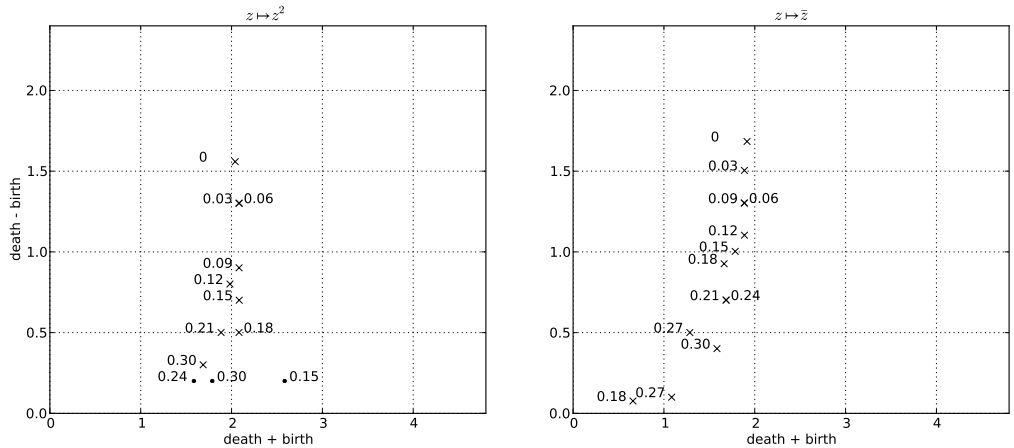

Figure 8: The superposition of the 1-dimensional persistence diagrams for $f(z) := z^2$ and $t = 2$ on the left and for $f(z) := \bar{z}$ and $t = -1$ on the right. The crosses are labeled by the level of the Gaussian noise used to generate the datasets. The dots are labeled similarly, but they alert us of the fact that these persistence intervals occur for all values of t.

for not necessarily square matrices is not well understood. A relevant unpublished manuscript is [4], in which properties of the solution are discussed and a reduction algorithm is given.

3 Cohomology of recurrent systems

3.1 Persistent Cohomology and recurrent systems

Recurrence and periodicity are fundamental to dynamical systems observed in nature. We present vignettes of three types of behavior which can be studied using our topological framework. We give an archetypal example of a system of each kind, and show how our methods detect the behavior with little or no prior knowledge of the underlying phase-space or system. The minimum we require is a collection of samples from a 1-dimensional time-dependent signal.

3.1.1 Background

At the heart of our method is a technique of Takens, which we use to boost the topological signal:

Definition 3.1. *Give a time-series $f : t \to \mathbb{R}$, a* **time-delay embedding** *is a lift to a time-series $\phi : t \to \mathbb{R}^d$ defined by*

$$\phi(t) = (f(t), f(t+\alpha), \ldots, f(t+(d-1)\alpha))$$

Takens' proved a remarkable theorem about these embeddings [62, 61] :

Theorem 3.2. *Let $\mathcal{M}$ be compact manifold of dimension m. For pairs (ϕ, y) with $\phi \in \mathrm{Diff}^2(\mathcal{M})$, $y \in C^2(\mathcal{M}, \mathbb{R})$, it is a generic property that the map $\Phi_{(\phi,y)} : \mathcal{M} \to \mathbb{R}^{2m+1}$ defined by*

$$\Phi(x)_{(\phi,y)} = (y(x), y(\phi(x)), \ldots, y(\phi^{2m}(s)) \tag{29}$$

is an embedding;

The theorem states that almost every time-delay embedding of a 1-dimensional measurement (time-series) can recover the underlying manifold and the dynamics of the system.

This is **Step 1** of our contribution: using the time-delay embedding we lift the signal to d-dimensions, the points of the lifted signal then clustering around some submanifold or other subspace of $\mathbb{R}^d$. Takens' theorem gives a necessary condition for this submanifold to recreate the full phase space from an idealized continuous signal; but we are faced with finite noisy data, so we must choose parameters a little more carefully for a 'good' embedding.

The original 1-dimensional signal is now a path in a higher-dimensional phase space. Periodic and recurrent behavior is characterized by the path returning to itself, creating one or more loops, that is to say topological *circles*. For example, the simplest periodic system is a sinusoid, which precisely traces out a circle in phase space. The circle is not present in the 1-dimensional signal, but appears upon boosting to 2 dimensions by a delay embedding $\{t \mapsto (\sin(t), \sin(t+a))\}$.

Step 2 is to use persistent cohomology to detect these circles, or rather *co-circles*: coordinate functions from the phase space to the standard unit circle. A well-known result in algebraic topology asserts that co-circles are classified (up to homotopy) by 1-dimensional cohomology.

$$\mathrm{H}^1(\mathbb{X}; S^1) \cong [\mathbb{X}, S^1]$$

As an outline we give the following steps:

1. Given a point cloud in a metric space compute the persistent cohomology of the Vietoris-Rips filtration.
2. Choose a persistent cohomology class and a scale based on the persistence diagram.
3. Find the harmonic representative of this class at the scale using least squares - which is gives an angle valued function on the data points.

We refer the reader to [55] for details of how this is done.

Since we are working with finite noisy data, we use topological persistence to identify the most robust of these coordinates. Each co-circle is associated to a point in the persistence diagram whose position indicates its robustness. As a useful side-effect, this can be used as a proxy for the quality of the Takens embedding; we can tune the delay parameters to maximize robustness.

Step 3 is to observe the dynamics in the new circular coordinates. We shall see how to obtain qualitative and quantitative information about periodic, quasiperiodic, and recurrent dynamical systems.

3.1.2 Pipeline

For a fixed choice of parameters ℓ and d, we embed the time-series at hand into $\mathbb{R}^d$.

Next we construct a simplicial complex approximating the topology of the embedded point cloud. For instance, the Vietoris–Rips construction produces a filtered simplicial complex reflecting the topology of the data at different scales. This is efficient even for very high embedding dimension d. For more details, we refer the reader to [55].

From this we construct a persistence diagram for 1-dimensional cohomology. This distinguishes high- and low-relevance topological features. The 'gap' between them is analogous to a signal-to-noise ratio [54], which can be used to tune the delay embedding and other parameters.[7]

[7] There are many other ways to choose good parameters, including recent statistical methods [60, 57, 52, 58, 59].

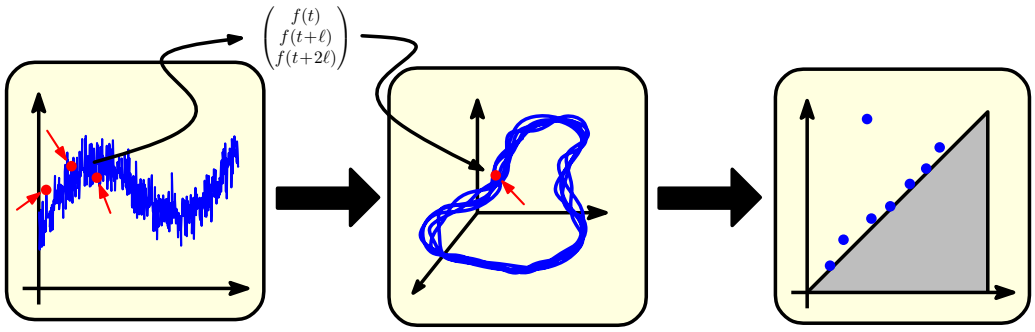

Figure 9: The first step is to choose parameters and compute a time-delay embedding. The persistence diagram of a distance filtration gives a natural measure of the quality of the embedding based on which we can change the time-delay parameters.

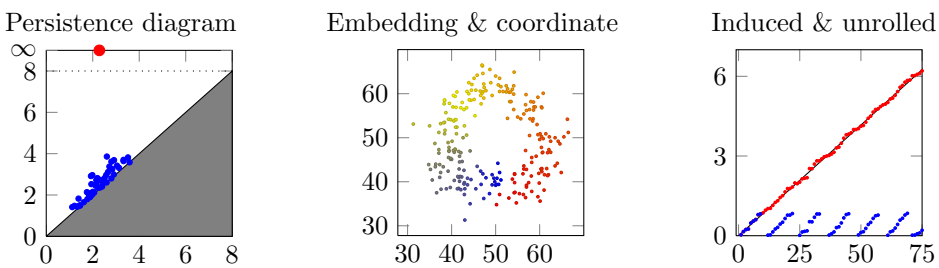

Figure 10: Monthly rainfall measurements from Nottingham [56]. On the right, we unroll the coordinate and fit a linear model. Computing the slope in the unrolled coordinate yields 1/12.002 with a correlation of 0.9995.

From the diagram we then choose one or several high-relevance persistent 1-cocycles and construct their circular coordinates using harmonic smoothing (see [55]).

3.1.3 Models of Behaviour

We describe three types of behavior along with their corresponding topological models.

—Periodic systems correspond to a circle $\mathbb{S}^1$.

—Quasiperiodic systems are modeled by a k-dimensional torus $\mathbb{T}^k = (\mathbb{S}^1)^k$. For instance a system with two periods will trace out a trajectory on a torus $\mathbb{T}^2$. Depending on the ratio of the periods, the trajectory will be a dense curve on the torus or a torus knot. Circular coordinates on the torus can be exploited to extract this periodicity information, in a sort of 'topological Fourier analysis.'

—Recurrent systems are modeled by a bouquet of circles $\mathbb{S}^1 \vee \cdots \vee \mathbb{S}^1$. The archetypal example is the Lorenz system. Its dynamics circulate repeatedly around the two wings of a butterfly-shaped attractor in an aperiodic sequence.

Periodic Systems The phase space of a periodic system is a topological circle, and our methods give a coordinate mapping x from this circle to a standard circle. We can use this to recover the

period of the system. The first step is to plot the time series in terms of the circular coordinate $x = x(t)$, as in Figure 10. The second step is to remove the discontinuities to get a continuous real time series $\bar{x}(t)$, a classic problem in signal processing known as *phase unwrapping*. For discrete times series this can be done using the heuristic

$$\bar{x}(i) = \left\lfloor \bar{x}(i-1) - x(i) + \tfrac{1}{2} \right\rfloor + x(i) \tag{30}$$

There is also a topological unwrapping procedure which is more resistant to noisy sampling. To explain this, note that the circular coordinate is constructed from a 1-cocycle α with integer coefficients (each directed edge typically taking values 0, 1, -1). This is then smoothed to a real cocycle $\tilde{\alpha} = \alpha + d\hat{x}$ with minimal ℓ_2-norm, and x is defined to be the fractional part of $\hat{x}$. The correct lift for each edge ij is given by the expression $\tilde{\alpha}(ij)$, which we can retain for this purpose.

Once the phase has been unwrapped, period recovery becomes a matter of classical regression. We can fit the best line according to whatever criteria we desire; in the examples below we use classical ℓ_2-minimization. As a proof-of-concept, we show the procedure on average monthly rainfall data taken over 30 years in Nottingham, England [56]. We recover a period of 12, indicating that a year indeed has 12 months (Figure 10).

Quasi-Periodic Systems The signal $f(t) = \sin(\alpha t) + \sin(\beta t)$ can be thought of as the composition of a path $t \mapsto (\alpha t, \beta t)$ into a torus, with a real function defined on the torus $(x, y) \mapsto \sin(x) + \sin(y)$. It follows that if α/β is irrational then the path will over time occupy a dense subset of the torus. Thus the entire torus is the natural phase space for the signal.

Under a successful delay embedding (into at least 3, but preferably at least 4 dimensions) our framework produces two robust co-circles if the time series has been sampled long enough for the path to become dense in the torus. One can recognize this by considering the correlation plot of the two coordinates: the data will appear dense in the square (i.e. torus) generated by the two coordinates. More technically, one can compute the cohomology cup product of the two 1-cocycles. A non-zero cup product suggests this kind of quasiperiodic behaviour.

If the ratio α/β is rational, then the phase space is a circle embedded as a torus knot on the torus. Such a phase space may manifest differently at different scales: at small scales it will appear to be a circle (if the sampling is fine enough), and at larger scales it will appear as a torus. Persistent topology is well suited for discovering this sort of multi-scale geometry.

Recurrent Systems The archetypal example of chaotic recurrent behavior is the Lorenz attractor. Under a range of parameters, the system traces out a 'butterfly' in observation space (Figure 11), travelling around the two 'wings' in an aperiodic sequence. The sequence is not predictable in the long term, being unstable under small perturbations. However this description of the behavior is qualitatively stable.

We can discover this very easily using our methods. We generate a point-cloud data set near the attractor by following an arbitrary trajectory for a while. Persistent cohomology indicates two significant cocycles, from which we construct two co-circles. The time series can now be viewed in these circular coordinates.

The first observation is that the correlation plot of the two coordinates is clustered on a 'cross' in the coordinate square, or more precisely a bouquet of two circles in the coordinate torus. This is quite different from the quasiperiodic case, where the values taken by the two coordinates eventually fill the entire torus. We can now track the motion of the trajectory against time. At most one

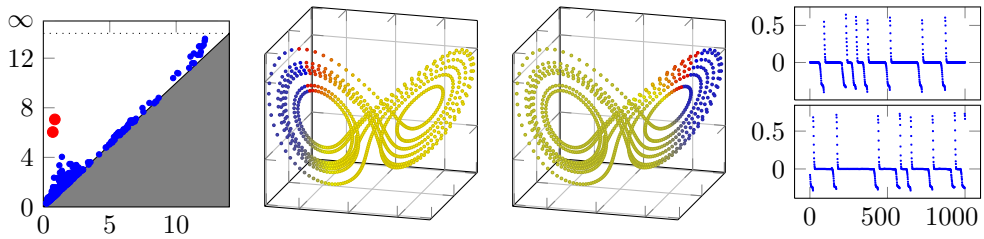

Figure 11: The Lorenz attractor. To the left, the persistence diagram from the point cloud we computed, with the chosen cocycles marked in large red dots. The resulting coordinates are indicated left to right, with their corresponding coordinate functions on the time series top to bottom in the right-most plot. The recurrent structure can be clearly seen in the pulse behaviour at the far right.

coordinate is 'active' at any given time, because the signal moves along at most one circle at a time. Each complete journey around that circle appears as a 'pulse' in the time series in that coordinate. The famous aperiodic behavior of the Lorenz system is immediately apparent from the time series in the two coordinates.

We emphasize that this heuristic conclusion can be reached with essentially no prior knowledge about the Lorenz system, and without direct reference to the butterfly.

3.1.4 Comments

Our approach to dynamical systems combines recent work in computational topology with well-known tools from nonlinear systems. Our methods are very general, since they are topological in nature. We have focused on the case of a time-series signal in one real dimension (or three, for the Lorenz system). In fact, the signal may take values in any metric space, even one with no natural coordinates of its own. The construction of the simplicial complex, its persistence and its co-circles depends only on this metric information. If the signal exhibits any 1-dimensional cohomology (perhaps after being boosted by a Takens embedding), then our method constructs circular coordinates through which the signal becomes amenable to quantitative and qualitative analysis.

3.2 A topological approach to the algorithmic computation of the Conley index of Poincaré operators

The rapid development of rigorous computational topological dynamics in the last twenty years brought many achievments. For some examples see [37, 24, 25, 26, 36, 45] and the references therein. The combination of advanced tools in topological dynamics with the algorithmic approach provides a detailed and rigorous description of concrete dynamical systems in applied and technical sciences. This is in contrast to both analytic methods and classical numerics. The analytic methods, perfect for the general theoretical description, often fail for concrete, non-toy systems due to the amount of computations needed. On the other hand classical numerics may not be reliable, providing spurious or ghost solutions. Such examples have been well documented in the literature (see [31, 33, 32] or [49] and the references within).

As with most new methods, rigorous computational topological dynamics brings not only

achievements but also many new challenges. One of the crucial barriers of the method is the algorithmic computation of the Conley index of Poincaré maps in differential equations. The knowledge of this index is useful in determining the recurrent behaviour of trajectories, in particular to establish the existence of periodic orbits or chaotic invariant sets. The computation is expensive, because the standard algorithm requires rigorous long time integration of the differential equations. In case of differential equations with strong expansion this is often prohibitive. Recently, a method to overcome this difficulty has been presented in [42]. The method is based on the concept of isolating segments introduced in [48]. The isolating segment is a special case of the concept of isolating block, the crucial tool in the classical construction of the Conley index for flows [27]. An alternative construction is based on the concept of index pair [28].

The method of [42] provides results but is painful in implementation, because each individual case requires manual construction of isolating segments. Roughly speaking, this is related to the fact that verifying algorithmically that a given polytope is an isolating block is possible but we have no useful algorithms constructing isolating blocks.

On the other hand, algorithms constructing index pairs for discrete dynamical systems are available and reasonably efficient [50, 34, 41].

On theoretical side, the computation of the Conely index for flows may be replaced by the computation of the Conley index for the t-translation operator of the flow [39]. The algorithmic version of the result is less general [43, 44] and requires some caution [38] but may be used fruitfully. Thus, a natural step is to apply an analogous approach for the computation of the Conley index of a Poincaré map. Though the theoretical side is surprisingly complicated, the algorithms based on this approach work as expected: they do not require a long time integration along the trajectories of the flow and benefit from the general algorithms computing index pairs for discrete dynamical systems.

3.2.1 Preliminaries

Let $k = 1, 2, \ldots$. For a map $f\colon X \to X$ we denote by f^k its k-th iterate, i.e.

$$f^k := f \circ \ldots \circ f \ (k\text{-times}).$$

We put also $f^0 :=$ identity and, if f is injective, $f^{-k} := (f^{-1})^k$. By an *Euclidean space* here we mean a finite-dimensional vector space over $\mathbb{R}$.

In the paper $\mathbb{F}$ denotes a fixed field. In the sequel the notion "vector space" or "linear space" refers to a vector space over $\mathbb{F}$. We write $V \cong W$ if the vector spaces V and W are isomorphic. We identify an endomorphism of $\mathbb{F}^k$ with its matrix in the canonical basis, i.e. for a k-dimensional square matrix $A = [a_{ij}]$,

$$A(e_j) = \sum_j a_{ij} e_i,$$

where $e_i := (0, \ldots, \overset{(i)}{1}, \ldots, 0) \in \mathbb{F}^k$. By a *graded vector space* we mean a sequence $V = \{V_n\}_{n\in\mathbb{Z}}$ of vector spaces. We identify V with the direct sum of V_n, i.e.

$$V = \bigoplus_{n\in\mathbb{Z}} V_n.$$

V is of *finite type* —— The vector space V is of *finite type* if V_n is finite-dimensional for all n, $V_n = 0$ for all $n < 0$ and for almost all $n \geqslant 0$. By a graded linear map between graded vector

spaces V and W we mean a sequence $\phi := \{\phi_n\}$ of linear maps $\phi_n \colon V_n \to W_n$. We identify ϕ with the cartesian product of maps ϕ_n restricted to $\bigoplus V_n \to \bigoplus W_n$. Assume V is of finite type and let ϕ be a graded linear endomorphism $V \to V$. The *Lefschetz number* of ϕ is defined as

$$\Lambda(\phi) := \sum_{n=0}^{\infty} (-1)^n \operatorname{trace} \phi_n.$$

Assume $V_n = 0$ for $n > n_0$ and for $n = 0, \ldots, n_0$ let $A(n) = [a(n)_{ij}]$ be the matrix of ϕ_n with respect to a given basis. We call $A = \operatorname{diag}[A(1), \ldots, A(n_0)]$ a matrix of ϕ. In particular,

$$\Lambda(\phi) = \Lambda(A) = \sum_{n=0}^{n_0} (-1)^n \sum_{i=0}^{\dim V_n} a(n)_{ii}.$$

3.2.2 Retractors

The objects of the *category of endomorphism* are linear maps $a \colon A \to A$ and the morphism between a and $b \colon B \to B$ are the linear maps $f \colon A \to B$ such that $f \circ a = b \circ f$. If f is an isomorphism, we call a and b *conjugated* and write $a \cong b$ to indicate it. By a *conjugacy class* we mean an equivalence class in the relation $\cong$.

By a *retractor* we mean a covariant functor on the category of endomorphisms of vector spaces which "retracts" endomorphisms onto automorphisms; i.e. restricted to the class of all automorphisms it is equal to the identity.

Let R be a retractor.

Proposition 3.3. *Let $a \colon A \to A$ and $b \colon B \to B$ be endomorphims. Assume there exist linear maps $f \colon A \to B$ and $g \colon B \to A$, and a number $r \geqslant 1$ such that the diagrams*

$$\begin{tikzcd} A \arrow[r, "a"] \arrow[d, "f"'] & A \arrow[d, "f"] \\ B \arrow[r, "b"] & B \end{tikzcd}$$

and

$$\begin{tikzcd} A \arrow[rr, "a^r"] \arrow[d, "f"'] & & A \arrow[d, "f"] \\ B \arrow[r, "g"] \arrow[rr, bend right, "b^r"'] & & B \end{tikzcd}$$

are commutative. Then $Ra \cong Rb$.

3.2.3 Topology

Let (X, A) be a topological pair. The *quotient space* X/A is defined as a set $(X \backslash A) \cup \{*\}$, where $*$ is equal to the set A. The *quotient map* is the identity on $X \backslash A$ and sends the points of A onto $*$. X/A is endowed with the *quotient topology*, i.e. a map $X/A \to Y$ is continuous if and only if its composition with q is continuous. In particular, $X/\varnothing = X \cup \{*\}$ has the topology of disjoint union. If $x \in X$, $[x]$ denotes x if $x \in X \backslash A$ and $*$ if $x \in A$.

A topological space is called a Euclidean neighborhood retract (shortly: ENR) if it is homeomorphic to a neighborhood retract in a Euclidean space.

3.2.4 Homology

We denote by H and $\check{H}$ the singular and, respectively, Čech homology functor with coefficients in the field $\mathbb{F}$. In te sequel we are interested mainly in the Euclidean space. In that case $\check{H}$ satisfies the exactness axiom (hence all the axioms of homology theory; c.f. [30], Chap. IX, Theorem 7.6) and for such a pair (X, A) one has

$$\check{H}(X, A) = \operatorname{inv}\lim H(U, V),$$

where the limit is taken over the inverse system of inclusions between pairs of open neighborhoods (U, V) of (X, A) in the Euclidean space. It follows there is a natural graded linear homomorphism

$$\mu := \mu_{(X,A)} \colon H(X, A) \to \check{H}(X, A)$$

induced by inclusions (c.f. [29], VIII.13.14).

Proposition 3.4. *If (X, A) is a pair of ENR-s then μ is an isomorphism.*

We consider singular homology theory based on simplexes. Recall, that for $d \in \mathbb{N}$ a *standard d-dimensional simplex* is the set $\Delta_d := \{x \in \mathbb{R}^{d+1} \colon \sum_i x_i = 1,\ x_i \geqslant 0\}$. A d-dimensional *singular simplex* on a topological space X is a continuous map $\Delta_d \to X$. A *chain* is a formal linear combination $\sum_i a_i\sigma_i$, where $a_i \in \mathbb{F}$ and σ_i are singular simplexes of the same dimension. A chain is called d-dimensional provided all σ_i are d-dimensional. The *support* of a d-dimensional chain $c := \sum_i a_i\sigma_i$, $a_i \neq 0$, is defined as

$$|c| := \bigcup_i \sigma_i(\Delta_d).$$

The *group of chains* on X is denoted by $S(X)$ (actually, in our considerations it is a graded vector space over $\mathbb{F}$). By ∂ we denote the *boundary operator* $S(X) \to S(X)$. A continuous map $f \colon X \to Y$ induces the *chain map* $S(f) \colon S(X) \to S(Y)$. If $A \subset X$ (i.e. (X, A) is a *topological pair*), we treat $S(A)$ as a subspace of $S(X)$ (i.e. if $c \in S(X)$ and $|c| \subset A$ then we regard c also as an element of $S(A)$). By the *group of cycles* on (X, A) we mean

$$Z(X, A) := \{z \in S(X) \colon \partial z \in S(A)\}.$$

The homology class of a cycle z is denoted by $[z]$. Recall that $[z] = [z']$ provided there exist $w \in S(X)$ and $a \in S(A)$ such that

$$\partial w = z - z' + a.$$

The chain map $S(f)$ induced by a continuous map $f \colon (X, A) \to (Y, B)$ transforms $Z(X, A)$ to $Z(Y, B)$.

3.2.5 Isolated invariant sets and Conley index

Local dynamical systems Throughout the rest of the paper we assume that X is a locally compact space. By a *continuous local dynamical system* (shortly: a *continuous system*) on X we mean a continuous map $\phi \colon D \to X$, where D is an open subset of $X \times \mathbb{R}$, such that for every $x \in X$,

(D1) the set

$$D_x := \{t \in \mathbb{R} \colon (x, t) \in D\}$$

is an interval containing 0,

(D2) $\phi(x,0) = x$,

(D3) if $t \in D_x$ then $s \in D_{\phi(x,t)}$ if and only if $s + t \in D_x$ and

$$\phi(x, t+s) = \phi(\phi(x,t), s).$$

Frequently we write $\phi_t(x)$ instead of $\phi(x,t)$ and if $A \subset X$ and $J \subset \mathbb{R}$ we write $\phi(A,J)$ instead of $\phi(A \times J)$.

A *discrete local dynamical system* (or shortly: a *discrete system*) on X is a map $f\colon U \to X$ such that U is an open subset of X and f is homeomorphism onto its image $f(U)$.

In the case $D = X \times \mathbb{R}$ the system ϕ is called *global* (or called a *continuous dynamical system*). Similarly, f is called a *global system* if it is a homeomorphism $X \to X$.

Let $S \subset X$. S is called *invariant* for a continuous system $\phi\colon D \to X$ (a discrete system $f\colon U \to X$) if for every $x \in S$, $D_x = \mathbb{R}$ and $\phi_t(S) = S$ for $t \in \mathbb{R}$ (respectively, if $S \subset U$ and f maps homeomorphically S onto S).

Let $\phi\colon D \to X$ be a continuous system and let $x \in X$ be such that $[0,\infty) \subset D_x$. The *ω-limit set* of x is defined as

$$\omega(x) := \bigcap_{t \geqslant 0} \mathrm{cl}(\phi(\phi_t(x), [0,\infty))).$$

Isolated invariant sets Let $A \subset X$. Let $\phi\colon D \to X$ be a continuous system and let $f\colon U \to X$ be a discrete one. By the *invariant part* of A (denoted $\mathrm{Inv}(A)$ or, more precisely, $\mathrm{Inv}_\phi(A)$ and $\mathrm{Inv}_f(A)$, respectively) we mean the maximal compact invariant set contained in A. An invariant set S is called *isolated* if it is equal to the invariant part of some its neighborhood N. Such an N is then called an *isolating neighborhood* (for S) provided it is compact. Let $\phi'\colon D' \to X'$ be another continuous system and let S and S' be isolated invariant sets for ϕ and, respectively, ϕ'. We call (S,ϕ) and (S',ϕ') *conjugated* and write it as

$$(S,\phi) \cong (S',\phi')$$

if there exist neighborhoods N of S and N' of S', and a homeomorphism $h\colon N \to N'$ such that for every $x \in N$,

$$\begin{aligned}&(t,x) \in D,\ \phi(x,[0,t]) \in N \iff (t,h(x)) \in D',\ \phi'(h(x),[0,t]) \in N',\\ &\phi'_t(h(x)) = h(\phi_t(x)).\end{aligned}$$

Similarly,

$$(S,f) \cong (S',f')$$

for discrete systems f and $f'\colon U' \to X'$ if there exist neighborhoods $N \subset U$ of S and $N' \subset U'$ of S', and a homeomorphism $h\colon N \to N'$ such that for every $x \in N$; $f(x) \in N$ if and only if $f'(h(x)) \in N'$ and $f'(h(x)) = h(f(x))$.

Index pairs and maps In this subsection we assume (N,L) is a pair of compact subsets of X. Let ϕ be a continuous system on X. (N,L) is called an *index pair for ϕ* if

(IP1) $\mathrm{cl}(N \backslash L)$ is an isolating neighborhood and

$$\mathrm{Inv}(\mathrm{cl}(N \backslash L)) \subset \mathrm{int}(N \backslash L),$$

(IP2) If $x \in L$ and $\phi(x, [0, t]) \subset N$ then $\phi(x, [0, t]) \subset L$,

(IP3) if $x \in N$ and

$$\phi(x, D_x \cap [0, \infty)) \not\subset N$$

then there exists $t \geqslant 0$ such that $\phi(x, [0, t]) \subset N$ and $\phi_t(x) \in L$.

An index pair (N, L) is called *regular* if the map

$$\sigma\colon N \to [0, \infty],\ \sigma(x) := \begin{cases} \sup\{t > 0\colon \phi(x, [0, t]) \subset N \backslash L\}, & \text{if } x \in N \backslash L, \\ 0, & \text{if } x \in L \end{cases}$$

(called the *exit-time map*) is continuous (compare [47, Definition 5.1]).

Assume now $f\colon U \to X$ is a discrete system on X and $L \subset N \subset U$. Define the *index map* $f_{N/L}\colon N/L \to N/L$ as

$$f_{N/L}([x]) := \begin{cases} f(x) & \text{if } x, f(x) \in N \backslash L, \\ * & \text{otherwise.} \end{cases}$$

It follows that $f_{N/L}(*) = *$. A criterion for continuity of the index map is given in [46, Theorem 4.3].

The pair (N, L) is called an *index pair for f* if (IP1) is satisfied and

$$N \cap f(L) \subset L, \tag{DIP2}$$

$$N \cap f^{-1}(X \backslash N) \subset L. \tag{DIP3}$$

It is easy to prove the following result (compare [46, Corollary 4.4]):

Proposition 3.5. *If (N, L) is an index pair for f then $f_{N/L}$ is continuous.* □

If (N, L) satisfies (IP1) and the index map $f_{N/L}$ is continuous, it is called a *Robbin-Salamon index pair* (shortly: an RS-pair). By Proposition 3.5, if (N, L) is an index pair, it is also an RS-pair.

If S is an isolated invariant set for ϕ (or f) and $S = \mathrm{Inv}(\mathrm{cl}(N \backslash L))$, w call (N, L) an *index pair* for (S, ϕ) (for (S, f), respectively).

Homology Conley index for discrete systems Assume X is metrizable. Let R be a fixed retractor. If (N, L) is an RS-pair for (S, f) then $\mathrm{CH}(S, f)$, the *homology Conley index* of (S, f) (over $\mathbb{F}$), is defined as the conjugacy class of the automorphism

$$R\check{H}(f_{N/L})\colon R\check{H}(N/L, *) \to R\check{H}(N/L, *).$$

One can prove that every neighborhood of S contains an index pair for (S, f) and the definition of the index is independent of the choice of an RS-pair. A proof of the latter statement can be based on Proposition 3.3 and the following result:

Proposition 3.6. *Let (N, L) and (N', L') be RS-pairs for (S, f), $(N, L) \subset (N', L')$, and let i denote the map $N/L \to N'/L'$ induced by the inclusion. Then the diagram*

$$\begin{tikzcd} N/L \arrow[r, "f_{N/L}"] \arrow[d, "i"'] & N/L \arrow[d, "i"] \\ N'/L' \arrow[r, "f_{N'/L'}"] & N'/L' \end{tikzcd}$$

is commutative. Moreover, there exists $r_0 \in \mathbb{N}$ *such that for every integer* $r \geqslant r_0$ *there exits a continuous map*

$$g\colon (N'/L', *) \to (N/L, *)$$

such that the diagram

$$\begin{tikzcd} N/L \arrow[r, "(f_{N/L})^r"] \arrow[d, "i"'] & N/L \arrow[d, "i"] \\ N'/L' \arrow[r, "g(f_{N'/L'})^r"] & N'/L' \end{tikzcd}$$

is commutative.

Proposition 3.7. *If* $(S, f) \cong (S', f')$ *then* $\mathrm{CH}(S, f) = \mathrm{CH}(S', f')$. □

Isolated invariant sets for a continuous system and its discretizations Let ϕ be a continuous system on X and let $h > 0$. The following proposition is proved in [39].

Proposition 3.8. *S is an isolated invariant set for ϕ if and only if it is an isolated invariant set for ϕ_h.*

3.2.6 Conley index of Poincaré maps

Periodic non-autonomuous equations Let V be a Euclidean space. For $A \subset \mathbb{R} \times V$ and $t \in \mathbb{R}$ put

$$A_t := \{x \in V : (t, x) \in A\}.$$

Let Ω be an open subset of $\mathbb{R} \times V$. Assume $f\colon \Omega \to V$ is a time-dependent vector-field such that the equation

$$\dot{x} = f(t, x) \tag{31}$$

has the uniqueness property of the initial-value problem

$$x(t_0) = x_0 \tag{32}$$

associated to (31) (for example, f is smooth). Denote by

$$t \to \Phi_{t_0,t}(x_0)$$

the solution of (31),(32). Let $T > 0$. In the sequel we assume Ω and f are T-periodic with respect to the first variable, i.e.

$$\begin{aligned} &\Omega_{t+T} = \Omega_t, \\ &f(t + T, x) = f(t, x) \end{aligned}$$

for $t \in \mathbb{R}$ and $(t, x) \in \Omega$. It follows, in particular, that

$$\Phi_{t_0,t} = \Phi_{t_0+T,t+T}.$$

We call

$$P := \Phi_{0,T}$$

the *Poincaré map* for the problem (31),(32). Its domain is equal to the set

$$\{x \in \Omega_0 \colon \Phi_{0,t}(x) \text{ is defined for all } t \in [0,T]\}.$$

Let $[t]$ denote the modulo-T class of $t \in \mathbb{R}$ in $\mathbb{R}/T\mathbb{Z}$ and let Σ denote the quotient space of Ω obtained by the identification of $t \times \Omega_t$ with $t + T \times \Omega_t$. Hence,

$$\Sigma = \bigcup_{t \in [0,T)} [t] \times \Omega_t \subset \mathbb{R}/T\mathbb{Z} \times V.$$

Thus, the equation (31) induces two continuous systems ϕ on Σ and ψ on Ω given by

$$\phi_t([\tau], x) = ([\tau + t], \Phi_{\tau,\tau+T}(x)),$$
$$\psi_t(\tau, x) = (\tau + t, \Phi_{\tau,\tau+T}(x)).$$

Proposition 3.9. *Let $S \subset \Sigma$. The following conditions are equivalent:*

(i) S is isolated invariant for ϕ,

(ii) S is isolated invariant for ϕ_h, for every $h > 0$,

(iii) S is isolated invariant for ϕ_h, for some $h > 0$,

(iv) S_0 is isolated invariant for the Poincaré map P and $S_t = \Phi_{0,t}(S_0)$ for each $t \in (0,T)$.

The main theorem Let $h > 0$ and let (N, L) be an index pair for ϕ_h. Put

$$S := \mathrm{Inv}_{\phi_h}(\mathrm{cl}(N \backslash L)).$$

By Proposition 3.9, S_0 is an isolated invariant set for the Poincaré map P. The main theoretical result of the present paper is

Theorem 3.10. *Let $T/h \in \mathbb{Q}$. Assume N_0 and L_0 are ENR-s,*

$$k := \dim H(N_0, L_0),$$

$A = [a_{ij}]$ is a graded $(k \times k)$-matrix over $\mathbb{F}$ and

$$\left(u_j, \sum_{i=1}^{k} a_{ij} u_i\right), \ j = 1, \ldots, k,$$

are h-movable pairs of contiguous cycles over $[0,T]$ such that $\{[u_j] \colon j = 1, \ldots, k\}$ is a basis of $H(N_0, L_0)$. Then $\mathrm{CH}(S_0, P)$ is equal to the conjugacy class of RA.

AAn example of application of Theorem 3.10 is the following

Corollary 3.11. *Under assumptions of Theorem* 3.10*, if*

$$\Lambda(A) \neq 0$$

then (31) *has a T-periodic solution.*

In Theorem 3.10, the assumption on h-movability is essential. Indeed, consider the equation

$$\dot{x} = 1$$

on $\mathbb{R}$. We treat it as T-periodic for some $T > 0$. Let $h = 2$ and for each $t \in \mathbb{R}$ let

$$N_t := [0,1] \cup [2,6], \; L_t := [4,6].$$

It follows (N, L) is an index pair for ϕ. Obviously, the invariant part of N is empty, hence the Conley index of the Poincaré map is trivial. On the other hand, let u be equal to the singular 0-dimensional simplex 1 in the interval $[0,1]$. Then u is a cycle which is equal to its homology class and it is a generator of $H(N_0, L_0) \cong \mathbb{F}$. Moreover, (u, u) is a pair of contiguous cyles. Indeed, the corresponding chains w and z can be given as w equal to the 1-dimensional singular simplex $[0,T] \times 1$ in $[0,T] \times [0,1]$ and $z = 0$. Note however, the pair (u, u) is not h-movable. Since $A = 1$, its conjugacy class is nontrivial.

Based on this we developed a rigorous algorithm, whose details we omit here. Please see the full paper of "A topological approach to the algorithmic computation of the Conley index of Poincare operators" (attached) for details.

3.2.7 Examples

We applied the algorithm above to the differential equation

$$\dot{z} = (1 + e^{i\eta t}|z|^2)\overline{z},$$

which shows chaotic behavior for $\eta \in (0,1]$ (see [42] and references therein). This equation has period $T = 2\pi/\eta$ in t. We analysed the equation for $\eta = 2.0$ using the parameter $h = 0.03$. We covered the candidate $M = S^1 \times [-3,3] \times [-3,3] = [\mathcal{M}]$ for an isolating neighborhood using cubes of equal size as described above. Our software found a combinatorial index pair $(\mathcal{N}, \mathcal{L})$ inside $\mathcal{M}$ at a refinement depth of $k = 6$. The chains constructed by our algorithm are shown in Figure 12.

One crucial property of the index pair is that the exit set has a certain thickness (in our case we used a thickness of 4 cubes) to have enough movable 1-cells in $\mathcal{L}$ along which to construct the chain z. This was achieved by first calculating the set $\mathrm{Inv}(\mathcal{M}, \mathcal{F})$, then thickening this set of cubes to a set $mathcalK$ with $\mathrm{Inv}(\mathcal{M}, \mathcal{F}) \subset mathcalK \subset \mathcal{M}$. Then immediately $\mathrm{Inv}(mathcalK, \mathcal{F}) = \mathrm{Inv}(\mathcal{M}, \mathcal{F})$ and we took as a combinatorial index pair $\mathcal{N} = \mathrm{Inv}^-(mathcalK, \mathcal{F}), \mathcal{L} = \mathrm{Inv}^-(mathcalK, \mathcal{F}) \backslash \mathrm{Inv}(\mathcal{M}, \mathcal{F})$.

Finding the weak index pair $(\mathcal{N}, \mathcal{L})$ took 110 seconds using a 2.4GHz CPU with 6 GB of RAM. Most of the time was used for constructing $\mathcal{F}_M$. The construction of the chains z, w and v took some seconds on our first implementation that is not yet optimized for speed. The set $\mathcal{M}$ consists of $(2^6)^3 = 262144$ cubes, the set $\mathcal{N}$ of 83746 cubes. Of course, we are only interested in the homology class $[v] \in H_1(N_0, L_0)$. Without using SHORTEN, we got a different 1-chain v', but with $[v] = [v']$ in $H_1(N_0, L_0)$.

Using Theorem 3.10, we see that the generator $[u] \in H_1(N_0, L_0)$ is sent to $-[u] \in H_1(N_0, L_0)$ under the endomorphism induced by the index map of the Poincaré map.

4 Hierarchies of maps

Persistent (co)homology, has been one of the central objects of study in applied and computational topology. Numerous extensions have been proposed to the original formulation including zig-zag

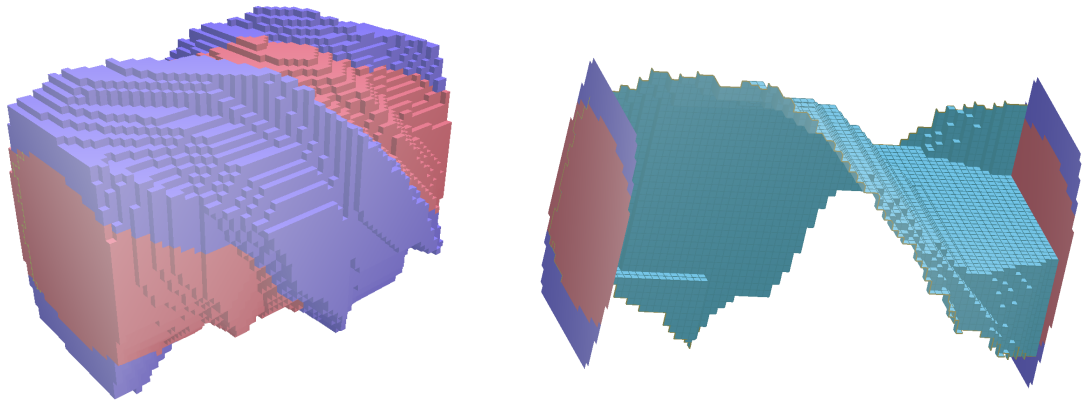

Figure 12: The left figure shows the full cubes in $(\mathcal{N}, \mathcal{L})$ and a representing 1-chain u of a generator $[u]$ of $H_1(N_0, L_0)$. The right figure shows the constructed 2-chain w in cyan. The constructed 1-chain $[2^k] \times v$ can be seen at the right edge. It is the image of $[u]$ under the endomorphism in homology induced by the index map of the Poincaré map.

persistence [72] and multi-dimensional persistence [71]. Whereas the original persistence looks at a filtration, an increasing sequence of space. Zig-zag persistence extended the theory and showed that the direction of the maps does not matter using tools from quiver theory. In multi-dimensional persistence, multifiltrations are considered. In this paper, we also look at the problem of persistence in more general diagrams using tools from lattice theory. There is another key difference in this work however. Rather than try to find a decomposition of the digram into indecomposables, we concentrate on pairs of spaces within diagrams addressing the more difficult problem of indecomposables in the sequel paper.

Lattice theory is the study of order structures and the deep connections between topology and lattice theory has been known since the work of Stone [83], showing an duality between Boolean algebras and certain topological spaces, called appropriately Stone spaces. In the first section of this paper we present the basic concepts of lattice theory. These preliminaries mostly refer to classical results on distributive lattices and Heyting algebras, and can be skipped by the reader that is familiar with the subject. A study of lattice theory and, in general, of universal algebra, can be found in [80], [81], [67] and [68].

A description of the topological background follows in the second section, reviewing the main concepts and results of Persistent Homology and suggesting several examples that are a motivation to this study. Good reviews on topological data analysis are given in [69] and [98], on persistent homology are given in [94] and [97], and on zig-zag persistence are given in [72], [70] and [90].

In the following section we describe the order structure of our diagrams by a partial order induced by certain maps between vector spaces, and show that this order provides a lattice structure. We construct the meet and join operations using the natural concepts of equalizers and coequalizers of linear maps, and show that this construction stabilizes. We shall see that the constructed lattice is a complete Heyting algebra, one of the algebraic objects of biggest interest in topos theory.

From the latter results we discuss connections with persistent homology, and give a different perspective on several aspects of this theory. In particular, we look at stability of persistence

diagrams and retrieve general laws both based on concrete examples (like standard or zig-zag persistence) and on the interpretation of laws derived from the lattice theoretic analysis. Finally we introduce a few algorithmic applications follow which we will develop further in a subsequent paper.

4.1 Preliminaries

A *lattice* is a partially-ordered set (or poset) expressed by $(L, \leqslant)$ for which all pairs of elements have an infimum and a supremum, denoted by $\wedge$ and $\vee$ respectively. These are also commonly known as the *meet* and *join*, which is the terminology we use in this paper. A lattice A can be seen as an algebraic structure $(L; \wedge, \vee)$ with two operations $\wedge$ and $\vee$ satisfying

(l1) *associativity*: $x \wedge (y \wedge z) = (x \wedge y) \wedge z$ and $x \vee (y \vee z) = (x \vee y) \vee z$,

(l2) *idempotence*: $x \wedge x = x = x \vee x)$,

(l3) *commutativity*: $x \wedge y = y \wedge x$ and $x \vee y = y \vee x$

(l4) *absorption*: $x \wedge (x \vee y) = x = x \vee (x \wedge y)$.

The equivalence between this algebraic perspective of a lattice L and its ordered perspective is given by the following equivalence: for all $x, y \in L$, $x \leqslant y$ iff $x \wedge y = x$ iff $x \vee y = y$. If every subset of a lattice L has a supremum and a infimum, L is named a *complete lattice*. A partial order is named *chain* (or *total order*) if every pair of elements is related, that is, for all $x, y \in A$, $x \leqslant y$ or $y \leqslant x$. Every chain is a lattice. On the other hand, an *antichain* is a partial order for which no two elements are related. Examples of lattices include the power set of A can be ordered by subset inclusion, the collection of all partitions of A ordered by refinement, or the Cartesian square of the natural numbers ordered by the natural order induced by the standard order of the natural numbers. With additional constraints on the operations we get different types of lattices. A lattice L is *distributive* if, for all $x, y, z \in S$, it satisfies one of the following equivalent equalities:

(d1) $x \wedge (y \vee z) = (x \wedge y) \vee (x \wedge z)$;

(d2) $x \vee (y \wedge z) = (x \vee y) \wedge (x \vee z)$;

(d3) $(x \vee y) \wedge (x \vee z) \wedge (y \vee z) = (x \wedge y) \vee (x \wedge z) \vee (y \wedge z)$.

The following result gives useful characterizations of the distributivity of a lattice L:

Proposition 4.1. *[67] A lattice L is distributive if and only if one of the following equivalent statements hold:*

(i) for all $x, y, z \in L$, $x \wedge y = x \wedge z$ and $x \vee y = x \vee z$ imply $y = z$;

(ii) L does not have embedded any copy of the diamond $\mathbf{M}_3$ or of the pentagon $\mathbf{N}_5$ determined by the Hasse diagrams below.

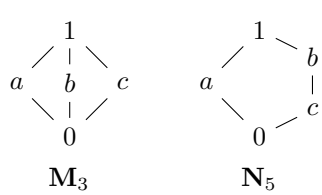

A *completely distributive lattice* is a complete lattice in which arbitrary joins distribute over arbitrary meets, i.e., if for any family $\{ x_{j,k} \}_{j \in J, k \in K_j}$ of L,

$$\bigwedge_{j \in J} \bigvee_{k \in K_j} x_{j,k} = \bigvee_{f \in F} \bigwedge_{j \in J} x_{j,f(j)}$$

where F is the set of choice functions f choosing for each index j of J some index $f(j)$ in K_j. A bounded lattice L is a *Heyting algebra* if, for all $a, b \in L$ there is a greatest element $x \in L$ such that $a \wedge x \leqslant b$. This element is the *relative pseudo-complement* of a with respect to b denoted by $a \to b$. A subalgebra of an Heyting algebra is thus closed to the usual lattice operations $\wedge$ and $\vee$, and to $\to$. Examples of Heyting algebras are the open sets of a topological space, as well as all the finite nonempty chains (that are bounded and complete). Furthermore, every complete distributive lattice L constitutes an Heyting algebra satisfying the identity

$$x \wedge \bigvee_{i \in I} y_i = \bigvee_{i \in I} (x \wedge y_i)$$

with the arrow operation given by

$$x \to y = \bigvee \{ x \in L \mid x \wedge a \leqslant b \}.$$

Complete Heyting algebras are a central object of the study of pointless topology.

4.2 Problem Statement

We motivate our constructions with the following examples: Let $\mathbb{X}$ be a space and $f : \mathbb{X} \to \mathbb{R}$ a real function. The object of study of persistent homology is a filtration of $\mathbb{X}$ – a monotonically non-decreasing sequence

$$\varnothing = \mathbb{X}_0 \subseteq \mathbb{X}_1 \subseteq \mathbb{X}_2 \subseteq \ldots \subseteq \mathbb{X}_{N-1} \subseteq \mathbb{X}_N = \mathbb{X}$$

To simplify the exposition, we assume that this is a discrete finite filtration of tame spaces. Taking the homology of each of the associated chain complexes, we obtain

$$\mathrm{H}_*(\mathbb{X}_0) \to \mathrm{H}_*(\mathbb{X}_1) \to \mathrm{H}_*(\mathbb{X}_2) \to \ldots \to \mathrm{H}_*(\mathbb{X}_{N-1}) \to \mathrm{H}_*(\mathbb{X}_N)$$

We take homology over a field k – therefore the resulting homology groups are vector spaces and the induced maps are linear maps. In [78], the $(i,j)-$*persistent homology groups* of the filtration are defined as

$$\mathrm{H}_*^{i,j}(\mathbb{X}) = \operatorname{im} \mathrm{H}_*(\mathbb{X}_i) \to \mathrm{H}_*(\mathbb{X}_j)$$

This motivates the idea for the construction of a totally ordered lattice. To see this, let us take as our set the homology groups with a partial order induces by the indexes of the spaces in the filtration. We can define two lattice operations $\wedge$ and $\vee$ as follows:

$$\mathrm{H}_*(\mathbb{X}_i) \vee \mathrm{H}_*(\mathbb{X}_j) = \mathrm{H}_*(X_{\max(i,j)})$$
$$\mathrm{H}_*(\mathbb{X}_i) \wedge \mathrm{H}_*(\mathbb{X}_j) = \mathrm{H}_*(X_{\min(i,j)})$$

With these operations we get a finite chain and, thus, a complete Heyting algebra (see this discussion in the following section). The definition of persistent homology groups can then be rewritten as follows:

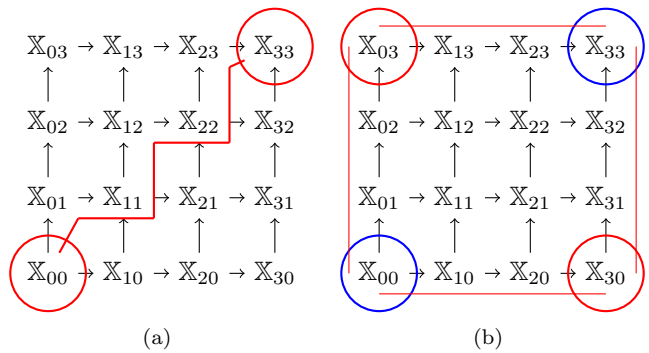

Figure 13: The lattice operations in the case of a bifiltration. (a) If the two elements are comparable, by the commutivity of the diagram we can choose any path to find the persistent homology groups. (b) If the elements are incomparable, we can find the smallest and largest elements where they become comparable. In both cases we recover the rank invariant of [71]

Definition 4.2. *For any two elements* $\mathrm{H}_*(\mathbb{X}_i)$ *and* $\mathrm{H}_*(\mathbb{X}_j)$*, the rank of the persistent homology classes is* $\operatorname{im} \mathrm{H}_*(\mathbb{X}_i \vee \mathbb{X}_j) \to \mathrm{H}_*(\mathbb{X}_i \wedge \mathbb{X}_j)$*.*

The case of a filtration, where a total order exists, does not have a very interesting underlying order structure. Let us now look at the case where we have more than one parameter. This is known as multidimensional persistence and has been studied in [71] and [73]. We shall start by looking at a bifiltration, i.e., a filtration on two dimensions (or parameters).
Observe that, for related elements of the filtration, these operations coincide with the ones defined above for the standard persistence case. However, when we consider incomparable elements, the meet and join operations are given by the rectangles they determine. Adjusting our definitions from above we can define the lattice operations in a natural way by setting:

$$\mathrm{H}_*(\mathbb{X}_{i,j}) \vee \mathrm{H}_*(\mathbb{X}_{k,\ell}) = \mathrm{H}_*(X_{\max(i,k),\max(j,\ell)})$$
$$\mathrm{H}_*(\mathbb{X}_{i,j}) \wedge \mathrm{H}_*(\mathbb{X}_{k,\ell}) = \mathrm{H}_*(X_{\min(i,k),\min(j,\ell)})$$

Note that, by the commutativity, any two elements which have the same meet and join define the same rectangle in the bifiltration, determined by the properties in the Hasse diagrams represented in Figure 13. By the assumed commutativity of the diagram, any path through the rectangle has equal rank and so the map of the meet to join gives the rank invariant of Definition 4.2.

Problem 4.3. *Given a commutative diagram of vector spaces and linear maps between them, we construct an order structure that completes it into a lattice, study its algebraic properties and develop algorithms based on this.*

Remark 4.4. *Quiver theory is also concerned with diagrams of vector spaces and linear maps. However, a key difference is that the diagrams in quiver theory are generally not required to be commutative.*

Remark 4.5. *We concentrate on the persistence between two elements rather than decomposition of the entire diagram. While we believe the constructions in this paper can aid this decomposition, it*

does not immediately follow. As such, any reference to a diagram should be understood as referring to the input collection of vector spaces and linear maps, rather than a persistence diagram.

4.3 Lattice Structure

Here we introduce the partial order and lattice operations to determine an order structure where the elements are vector spaces. The linear maps between them will define the relations between those vector spaces and limit concepts like equalizers and coequalizers (an equalizer is a set of arguments where a given family of maps have equal values, while a coequalizer is a generalization of a quotient by an equivalence relation) will serve us to define biggest and least elements.

4.4 Ordering Vector Spaces

Let us start by defining the equivalence of vector spaces A and B by: $A \leftrightsquigarrow B$ if there is an isomorphism between A and B. Without loss of generality we can quotient by this equivalence. In this case $A \oplus A = A$ and $A \oplus B = B \oplus A$. In the remainder of the paper we represent a monomorphism from A to B by $A \hookrightarrow B$, and a epimorphism from A onto B by $A \twoheadrightarrow B$.

Consider a directed acyclic graph of vector spaces G together with respective linear maps. Assume one unique component. This ordered structure is a poset regarding the following partial order: for all vector spaces A and B,

$$A \leqslant B \text{ if there exists a linear map } f : A \to B.$$

The identity map ensures the reflexivity of the relation: for all vector spaces A the identity map id_A provides the endorelation $\circlearrowleft A$. Transitivity is given by the fact that the composition of linear maps is a linear map and by the assumption that all diagrams are commutative. Antisymmetry is given by the fact that $A \leftrightarrows B$ implies $A \leftrightsquigarrow B$, that is, A and B are equal up to isomorphism: in detail, having the identity morphisms and usual composition of linear maps, the existence of linear maps $f : A \to B$ and $g : B \to A$ imply that $g \circ f = id_A$ and that $f \circ g = id_B$ as required.

Given A and C elements of the category of vector spaces $\mathcal{V}$, the *equalizer* $\mathcal{E}$ of a family of morphisms $\mathcal{F} = \{ f : A \to C \}$ is a pair (E, e) where E is a set (usually called *kernel set* of the equalizer) and $e : E \to A$ is a morphism in $\mathcal{V}$ such that $fe = ge$, for all $f, g \in \mathcal{F}$, with the following universal property: for any other morphism $e' : E' \to A$ in $\mathcal{V}$ such that $fe' = ge'$, for all $f, g \in \mathcal{F}$, there exists a unique morphism $\phi : E' \to E$ such that $e\phi = e'$. Dually, the *coequalizer* of $\mathcal{F}$ is a pair (H, h) where H is a set (usually called the *quotient set* of the coequalizer) and $h : A \to H$ is a morphism in $\mathcal{V}$ such that $hf = hg$, for all $f, g \in \mathcal{F}$, with the following universal property: for any other morphism $h' : A \to H'$ in $\mathcal{V}$ such that $h'f = h'g$, for all $f, g \in \mathcal{F}$, there exists a unique morphism $\phi : H \to H'$ such that $\phi h = h'$.

Given A and C elements of the category of vector spaces $\mathcal{V}$, the *equalizer* $\mathcal{E}$ of a family of morphisms $\mathcal{F} = \{ f : A \to C \}$ is a pair (E, e) where E is a set (usually called *kernel set* of the equalizer) and $e : E \to A$ is a morphism in $\mathcal{V}$ such that $fe = ge$, for all $f, g \in \mathcal{F}$, with the following universal property: for any other morphism $e' : E' \to A$ in $\mathcal{V}$ such that $fe' = ge'$, for all $f, g \in \mathcal{F}$, there exists a unique morphism $\phi : E' \to E$ such that $e\phi = e'$.

$$\begin{tikzcd}
E \arrow[r, "\mathrm{e}"] & A \arrow[r, shift left, "\mathrm{f}"] \arrow[r, shift right, "\mathrm{g}"'] & C \\
E' \arrow[u, dashed, "\phi"] \arrow[ur, "\mathrm{e'}"'] & &
\end{tikzcd}$$

Dually, the *coequalizer* of $\mathcal{F}$ is a pair (H, h) where H is a set (usually called the *quotient set* of the coequalizer) and $h : A \to H$ is a morphism in $\mathcal{V}$ such that $hf = hg$, for all $f, g \in \mathcal{F}$, with the following universal property: for any other morphism $h' : A \to H'$ in $\mathcal{V}$ such that $h'f = h'g$, for all $f, g \in \mathcal{F}$, there exists a unique morphism $\phi : H \to H'$ such that $\phi h = h'$.

$$\begin{tikzcd}
A \arrow[r, shift left, "\mathrm{f}"] \arrow[r, shift right, "\mathrm{g}"'] & C \arrow[r, "\mathrm{h}"] \arrow[dr, "\mathrm{h'}"'] & H \arrow[d, dashed, "\phi"] \\
& & H'
\end{tikzcd}$$

If $\mathcal{F} = \{ f, g, h, \dots \}$ its equalizer may be written as $eq(f, g, h, \dots)$ while its coequalizer is written as $coeq(f, g, h, \dots)$. Whenever $\mathcal{F} = \{ f \}$, the equalizer is (A, id_A) while the coequalizer is $(C/f(A), \pi_{f(A)})$. As for the degenerate case when $\mathcal{F} = \varnothing$, the equalizer is again (A, id_A) while the coequalizer is (C, id_C).

4.5 The lattice operations

In the following we will describe the construction of the operations $\wedge$ and $\vee$ based on the concept of direct sum, and a generalization of the concepts of equalizer and coequalizer.

Definition 4.6. *Let A and B be vector spaces, I and J be index sets and consider the sets of linear maps $\mathbb{F}_k = \{f_i : A \oplus B \to X_k \mid A, B \leqslant X_k, i \in I\}$ and $\mathbb{G}_k = \{g_i : Y_k \to A \oplus B \mid Y_k \leqslant A, B, i \in I\}$. Define $A \wedge B$ to be the kernel set $\mathcal{E}$ of the equalizer $eq(\oplus_{k \in I} \mathbb{F}_k)$ and, dually, $A \vee B$ to be the quotient set $\mathcal{C}$ of the coequalizer $coeq(\oplus_{k \in J} G_k)$.*

Intuitively, whenever A and B are vector spaces we construct $A \vee B$ as the limit of all vector spaces that have maps coming in from both A and B by gathering together all those maps to all vector spaces C_i above both A and B: in particular, this limit is the equalizer of such maps. Dually, we construct $A \wedge B$ as the colimit of all the linear maps going into A and B coming from a common vector space D_j. This intuition is represented in Figure 14. Hence, $A \wedge B$ is the limit of the $\{ A, B \}$-cone and $A \vee B$ is the colimit of the $\{ A, B \}$-cocone. Recall that (co)complete categories are the ones where the (co)limit of any diagram $F : I \to D$ exists. The category of vector spaces is both complete and cocomplete. Thus, we can generalize this to sets $\{ A_0, A_1, \dots, A_i, \dots \}$ in the sense of complete lattices.

The definitions for $\wedge$ and $\vee$ have a constructive nature that will show to be useful when we later describe the computation of the operations.

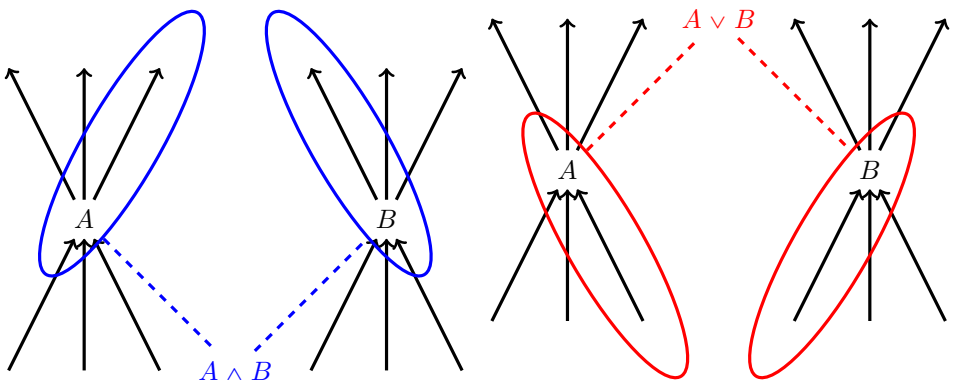

(a) meet operation $\wedge$ (b) join operation $\vee$

Figure 14: Intuition of the defined lattice operations meet, $\wedge$ and join, $\vee$.(a) Given two elements, A and B, the meet is defined by looking at all the spaces which A and B map into to compare them. (b) For the join, we use the dual construction and compare A and B using all the spaces which map into A and B.

Lemma 4.7. *Given vector spaces A and B there always exist vector spaces C and D such that $D \leqslant A, B \leqslant C$.*

Observe that $A \oplus B \cong A \oplus B/\Delta$ where $\Delta = \{ (x,x) \mid x \in A \oplus B \}$ is the minimal equivalence we can consider, while $\{ (0,0) \} \cong A \oplus B/\nabla$ where $\nabla = \{ (x,y) \mid x,y \in A \oplus B \}$ is the biggest equivalence considered. On the other hand, $\{ 0 \}$ can be seen as the kernel set determined by "too many" equations, while $A \oplus B$ is the kernel set determined by no equations.

A vector space is a *source* if it is no codomain of any map, and dually it is a *sink* if it in no domain of any map. According to the above in Lemma 4.7, the vector space $\{ 0 \}$ is a source and the vector space $A \oplus B$ is a sink.

Lemma 4.8. *Given vector spaces A and B there always exist $A \wedge B$ and $A \vee B$. Moreover,*

$A \wedge B$ is a subalgebra of $A \oplus B$;

$A \vee B$ is a quotient algebra of $A \oplus B$;

both of them constituting vector spaces.

Theorem 4.9. *Given vector spaces A and B, the construction of $A \wedge B$ and $A \vee B$ stabilizes.*

In the following result we will show that the elements of a commutative diagram of vector spaces together with the operations $\vee$ and $\wedge$ defined as above determine a lattice of vector spaces.

Theorem 4.10. *Let P be the set of elements of a diagram D. Then, the partially ordered set $(P; \leqslant)$ is a lattice of vector spaces for which the operations $\vee$ and $\wedge$ are defined as above.*

Corollary 4.11. *The persistence lattice is a complete lattice.*

4.6 Structural Consequences

In the following we describe some of the most relevant characteristics of the lattice that we have described in the earlier section. We shall see that, besides the algebraic properties due to its lattice nature, it is also modular and distributive. Let us first have a look at the properties of the operations $\wedge$ and $\vee$ given by the algebraic structure of the lattice above defined. It is not hard to see that the identity map implies that $A \wedge A = A$ and $A \vee A = A$. In fact, this algebraic property follows from the following:

Proposition 4.12. *A linear map $f : A \to B$ exists iff $A = A \wedge B$ iff $A \vee B = B$. Moreover, for all vector spaces A, B and C, the following equations are satisfied:*

(i) $(A \wedge B) \wedge C = A \wedge (B \wedge C)$ *and* $(A \vee B) \vee C = A \vee (B \vee C)$*;*

(ii) $A \wedge B = B \wedge A$ *and* $A \vee B = B \vee A$*;*

(iii) $A \wedge (A \vee B) = A$ *and* $A \vee (A \wedge B) = A$*.*

Lemma 4.13. *Let A and B be vector spaces. Then, $A \wedge B \to A \oplus B \to A \vee B$ is a short exact sequence.*

Remark 4.14. *Whenever A and B are vector spaces, Theorem 4.13 implies the isomorphism $A \vee B \cong A \oplus B/e(A \wedge B)$, where $e : A \wedge B \to A \oplus B$ is the equalizer map correspondent to the kernel set $A \wedge B$. Due to the definition of the operations $\wedge$ and $\vee$ above, this congruence reduces to*

$$A \oplus B/\{\, e(x) \mid f_i(x) = f_j(x) \,\} \cong A \oplus B/\langle (g_i(x), g_j(x) \rangle.$$

Theorem 4.15. *The persistence lattice is distributive.*

$$\begin{tikzcd}
 & X \vee A = X \vee B & \\
A \arrow[ur, "f"] & B \arrow[u, "u"] & X \arrow[ul, "s"'] \\
 & X \wedge A = X \wedge B \arrow[ul, "g"] \arrow[u, "v"] \arrow[ur, "t"'] &
\end{tikzcd}$$

Corollary 4.16. *The distributivity of the persistence lattice implies the existence of an isomorphism between $[A \wedge B, B]$ and $[A, A \vee B]$ using the maps $f : (A \vee B)/A \to B/(A \wedge B)$, $X \mapsto X \wedge B$, and $g : B/(A \wedge B) \to (A \vee B)/A$, $Y \mapsto A \vee Y$.*

Corollary 4.17. *The persistence lattice is completely distributive. Moreover, it constitutes a complete Heyting algebra.*

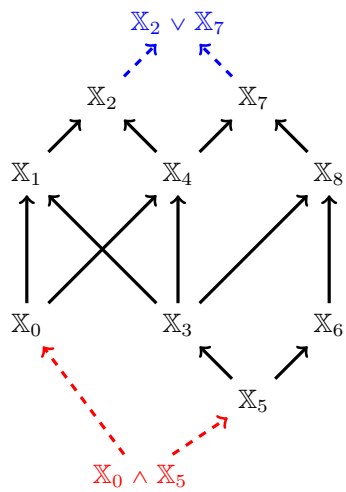

Figure 15: The lattice completion of a general diagram.

4.7 Largest Injective

The first application, we consider is the computation of the largest injective of a diagram. In principle, we are looking for something which persists over an entire diagram. Using the properties of the lattice, the largest injective must fulfill the be in the following images

$$\operatorname{im}\left(\mathrm{H}_*(\mathbb{X}_i) \wedge \mathrm{H}_*(\mathbb{X}_j) \to \mathrm{H}_*(\mathbb{X}_i) \vee \mathrm{H}_*(\mathbb{X}_j)\right) \qquad \forall i, j$$

By completeness, it follows that this can be written as

$$\operatorname{im}\left(\bigwedge_i \mathrm{H}_*(\mathbb{X}_j) \to \bigvee_i \mathrm{H}_*(\mathbb{X}_i)\right)$$

Using the order structure, we can rewrite the above as

$$\operatorname{im}\left(\bigwedge_{i \in \text{sources}} \mathrm{H}_*(\mathbb{X}_j) \to \bigvee_{j \in \text{sinks}} \mathrm{H}_*(\mathbb{X}_j)\right).$$

Recall that *sources* are all the elements in original diagram which are not the codomain of any maps and *sinks* are the elements which are not the domain of any maps.

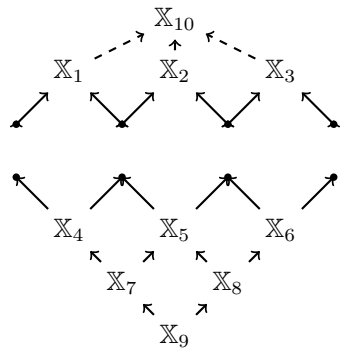

$$\operatorname{im}\left(\bigwedge_{i\in\text{sources}} \mathrm{H}_*(\mathbb{X}_j) \to \bigvee_{j\in\text{sinks}} \mathrm{H}_*(\mathbb{X}_j)\right)$$

References

[1] G. Carlsson and V. de Silva. Zigzag persistence. *Found. Comput. Math.* **10** (2010), 367–405.

[2] G. Carlsson, T. Ishkanov, V. de Silva and A. Zomorodian. On the local behavior of spaces of natural images. *Internat. J. Comput. Vision* **76** (2008), 1–12.

[3] F. Chazal, D. Cohen-Steiner, M. Glisse, L. J. Guibas and S. Y. Oudot. Proximity of persistence modules and their diagrams. *In* "Proc. 25th Sympos. Comput. Geom., 2009", 237–246.

[4] S. Cohen and C. Tomasi. Systems of bilinear equations. Techn. Rept., Dept. Comput. Sci., Stanford Univ., California, 1997.

[5] D. Cohen-Steiner, H. Edelsbrunner and J. Harer. Stability of persistence diagrams. *Discrete Comput. Geom.* **37** (2007), 103–120.

[6] D. Cohen-Steiner, H. Edelsbrunner, J. Harer and D. Morozov. Persistent homology for kernels, images, and cokernels. In "Proc. 20th Ann. ACM-SIAM Sympos. Discrete Alg., 2009", 1011–1020.

[7] C. Conley. *Isolated Invariant Sets and the Morse Index.* Amer. Math. Soc., CBMS Regional Conf. Series Math. **38**, 1978.

[8] H. Derksen and J. Weyman. Quiver representations. *Notices Amer. Math. Soc.* **52** (2005), 200–206.

[9] H. Edelsbrunner and J. L. Harer. *Computational Topology. An Introduction.* Amer. Math. Soc., Providence, Rhode Island, 2010.

[10] H. Edelsbrunner, D. Letscher and A. Zomorodian. Topological persistence and simplification. *Discrete Comput. Geom.* **28** (2002), 511–533.

[11] J. Gamble and G. Heo. Exploring uses of persistent homology for statistical analysis of landmark-based shape data. *J. Multivar. Analysis* **101** (2010), 2184–2199.

[12] A. Gyulassi, V. Natarajan, V. Pascucci, P.-T. Bremer and B. Hamann. A topological approach to simplification of three-dimensional scalar fields. *IEEE Trans. Visual. Comput. Graphics* (2006), 474–484.

[13] T. Kaczynski, K. Mischaikow and M. Mrozek. *Computational Homology.* Springer-Verlag, New York, New York, 2004.

[14] S. Kleene. *Introduction to Meta-Mathematics.* North Holland, Amsterdam, the Netherlands, 1952.

[15] S. MacLane. *Categories for the Working Mathematician.* Springer-Verlag, New York, New York, 1971.

[16] K. Mischaikow and M. Mrozek. The Conley index theory. In *Handbook of Dynamical Systems III: Towards Applications*, eds.: B. Fiedler, G. Iooss and N. Kopell, Elsevier, Singapore 2002, 393–460.

[17] M. Mrozek. Leray functor and the cohomological Conley index for discrete time dynamical systems. *Trans. AMS* **318** (1990), 149–178.

[18] M. Mrozek. Normal functors and retractors in categories of endomorphisms. *Univ. Jagiell. Acta. Math.* **29** (1992), 181–198.

[19] E. Spanier. *Algebraic Topology.* McGraw-Hill or Springer-Verlag, New York, 1966.

[20] S. Weinberger. What is ... persistent homology? *Notices Amer. Math. Soc.* **58** (2011), 36–39.

[21] A. Zomorodian. Fast construction of the Vietoris-Rips complex. *Computer and Graphics* **34** (2010), 263–271.

[22] A. Zomorodian and G. Carlsson. Computing persistent homology. *Discrete Comput. Geom.* **33** (2005), 249–274.

[23] CAPD::RedHom: reduction algorithms for homology computation. redhom.ii.uj.edu.pl.

[24] Z. Arai, H. Kokubu and P. Pilarczyk, Recent development in rigorous computational methods in dynamical systems, *Japan Journal of Industrial and Applied Mathematics*, **26**(2009) 393-417.

[25] Z. Arai, W. Kalies, H. Kokubu, K. Mischaikow, H. Oka, and P. Pilarczyk, A database schema for the analysis of global dynamics of multiparameter systems, *SIAM J. Applied Dyn Syst*, **8**(2009), 757–789.

[26] J. Bush, M. Gameiro, S. Harker, H. Kokubu, K. Mischaikow, I. Obayashi, P. Pilarczyk, Combinatorial-topological framework for the analysis of global dynamics, *Chaos*, **22**(2012), 047508.

[27] C. Conley, R. Easton, Isolated Invariant Sets and Isolating Blocks, *Trans. Amer. Math. Soc.*, **158** (1971), 35–61.

[28] C. Conley, Isolated invariant sets and the Morse index, *CBMS Regional Conference Series in Math* **38**(1978).

[29] A. Dold, Lectures on Algebraic Topology, Springer-Verlag, Berlin 1980.

[30] S. Eilenberg, N. Steenrod, Foundations of Algebraic Topology, Princeton University Press, Princeton 1952.

[31] D.F. Griffiths, P.K. Sweby, H.C. Yee, Spurious steady state solutions of explicit Runge-Kutta schemes, *IMA J. Num. Anal.*, **12** (1992), 319–338.

[32] J.K. Hale and H. Koçak, *Dynamics and Bifurcations*, Springer-Verlag, New York, 1991.

[33] A.R. Humphries, Spurious solutions of numerical methods for initial value problems, *IMA J. Num. Anal.*, **13** (1993), 263–290.

[34] T. Kaczynski, K. Mischaikow, M. Mrozek: Computational Homology, *Applied Mathematical Sciences*, Vol. 157, Springer-Verlag, 2004.

[35] W. D. Kalies, K. Mischaikow, R.C.A.M. VanderVorst: An algorithmic approach to chain recurrence, *Found. Comp. Math.*, **5** (2005), 409-449.

[36] E. Liz, P. Pilarczyk, Global dynamics in a stage-structured discrete-time population model with harvesting, *J. Theoret. Biol.*, **297**(2012), 148-165.

[37] K. Mischaikow, M. Mrozek, Chaos in Lorenz equations: a computer assisted proof, *Bull. Amer. Math. Soc. (N.S.)*, **33** (1995), 66–72.

[38] K. Mischaikow, M. Mrozek, F. Weilandt, An Algorithm for the Conley Index of a Flow in an Isolating Neighborhood, in preparation.

[39] M. Mrozek, The Conley index on compact ANR's is of finite type, *Results in Mathematics*, 18(1990),306-313.

[40] M. Mrozek, An Algorithmic Approach to the Conley Index Theory, *Journal of Dynamics and Differential Equations*, **11** (1999), 711-734.

[41] M. Mrozek, Index pairs algorithms, *Found. Comput. Math.* 6 (2006), 457–493.

[42] M. Mrozek, R. Srzednicki, Topological approach to rigorous numerics of chaotic dynamical systems with strong expansion, *Foundations of Computational Mathematics*, **10**(2010), 191–220,
DOI: 10.1007/s10208-009-9053-5.

[43] P. Pilarczyk, Computer assisted method for proving existence of periodic orbits, *Topological Methods in Nonlinear Analysis*, **13** (1999), 365-377.

[44] P. Pilarczyk, Topological-numerical approach to the existence of periodic trajectories in ODEs, *Discrete and Continuous Dynamical Systems 2003, A Supplement Volume: Dynamical Systems and Differential Equations*, 701-708.

[45] P. Pilarczyk, L. García, B.A. Carreras, I. Llerena, A dynamical model for plasma confinement transitions, *J. Phys. A: Math. Theor.*, **45**(2012), 125502.

[46] J.W. Robbin, D. Salamon, Dynamical systems, shape theory and the Conley index, Ergodic Theory Dynamical Systems 8* (1988), 375–393.

[47] D. Salamon, Connected simple systems and Conley index of isolated invariant sets, Trans. Amer. Math. Soc. 219 (1985), 1–41.

[48] R. Srzednicki, Periodic and bounded solutions in blocks for time-periodic nonautonomous ordinary differential equations, *Nonlinear Anal.*, **22** (1994), 707–737.

[49] A.M. Stuart, A.R. Humphries, *Dynamical Systems and Numerical Analysis*, Cambridge Univ. Press, Cambridge, 1998.

[50] A. Szymczak, A combinatorial procedure for finding isolating neighborhoods and index pairs , *Proc. Royal Soc. Edinburgh, Ser. A* **127A**(1997), 1075–1088.

[51] Computer Assisted Proofs in Dynamics, `http://capd.ii.uj.edu.pl/`.

[52] Liangyue Cao. Practical method for determining the minimum embedding dimension of a scalar time series. *Physica D: Nonlinear Phenomena*, 110(1–2):43 – 50, 1997.

[53] G. Carlsson. Topology and data. *American Mathematical Society*, 46(2):255–308, 2009.

[54] F. Chazal, L. J. Guibas, S. Y. Oudot, and P. Skraba. Persistence-based clustering in riemannian manifolds. In *Proceedings of the 27th annual ACM symposium on Computational geometry*, SoCG '11, pages 97–106, New York, NY, USA, 2011. ACM.

[55] V. de Silva, D. Morozov, and M. Vejdemo-Johansson. Persistent cohomology and circular coordinates. *Discrete and Computational Geometry*, 45(4):737—759, 2011.

[56] R. J. Hyndman. Time series data library. `http://data.is/TSDLdemo`. Accessed on 1.9.2012.

[57] H.S. Kim, R. Eykholt, and J.D. Salas. Nonlinear dynamics, delay times, and embedding windows. *Physica D: Nonlinear Phenomena*, 127(1–2):48 – 60, 1999.

[58] W. Liebert, K. Pawelzik, and H. G. Schuster. Optimal embeddings of chaotic attractors from topological considerations. *EPL (Europhysics Letters)*, 14(6):521, 1991.

[59] W. Liebert and H.G. Schuster. Proper choice of the time delay for the analysis of chaotic time series. *Physics Letters A*, 142(2–3):107 – 111, 1989.

[60] T. Sauer and J. A. Yorke. How many delay coordinates do you need? *International Journal of Bifurcation and Chaos*, 03(03):737–744, 1993.

[61] T. Sauer, J. A. Yorke, and M. Casdagli. Embedology. *Journal of Statistical Physics*, 65:579–616, 1991. 10.1007/BF01053745.

[62] F. Takens. Detecting strange attractors in turbulence. In David Rand and Lai-Sang Young, editors, *Dynamical Systems and Turbulence, Warwick 1980*, volume 898 of *Lecture Notes in Mathematics*, pages 366–381. Springer Berlin / Heidelberg, 1981. 10.1007/BFb0091924.

[63] M. Barr and C. Wells. *Category theory for computing science*, volume 10. Prentice Hall, 1990.

[64] A. Bauer, K. Cvetko-Vah, M. Gehrke, S. J. van Gool, and G. Kudryavtseva. A non-commutative priestley duality. *Topology and its Applications*, 2013.

[65] G. Bezhanishvili. Bitopological duality for distributive lattices and heyting algebras. *Mathematical Structures in Computer Science*, 20(3):359–393, 2010.

[66] N. Bezhanishvili. *Lattices of intermediate and cylindric modal logics.* Institute for Logic, Language and Computation, 2006.

[67] G. Birkhoff. *Lattice theory*, volume 5. AMS Colloquium Publications, Providence RI, third edition, 1940.

[68] S. Burris and H. P. Sankappanavar. *A course in universal algebra.* S. Burris and H. P. Sankappanavar, 1981.

[69] G. Carlsson. Topology and data. *Bulletin-American Mathematical Society*, 46(2):1–54, 2009.

[70] G. Carlsson, V. De Silva, and D. Morozov. Zigzag persistent homology and real-valued functions. In *Proceedings of the Annual Symposium on Computational Geometry*, pages 247–256, March 2009.

[71] G. Carlsson and A. Zomorodian. The theory of multidimensional persistence. *Discrete & Computational Geometry*, 42(1):71–93, 2009.

[72] G. Carlsson and V. de Silva. Zigzag persistence. *Found. Comput. Math.*, 10(4):367–405, 2010.

[73] G. Carlsson, G. Singh and A. Zomorodian. Computing Multidimensional Persistence. *arXiv.org*, July 2009.

[74] B. A. Davey and H. A. Priestley. *Introduction to lattices and order.* Cambridge University Press, 2002.

[75] R. P. Dilworth. A decomposition theorem for partially ordered sets. *Annals of Mathematics*, 51(1):161–166, 1950.

[76] A. Döring and C. Isham. A topos foundation for theories of physics: I. formal languages for physics. *Journal of Mathematical Physics*, 49, 2008.

[77] H. Edelsbrunner and J. L. Harer. *Computational Topology: An Introduction.* American Mathematical Society, 2010.

[78] H. Edelsbrunner, D. Letscher, and A. Zomorodian. Topological persistence and simplification. *Discrete & Computational Geometry*, 28(4):511–533, December 2012.

[79] J. D. Farley. The automorphism group of a function lattice: A problem of jónsson and mckenzie. *Algebra Universalis*, 36(1):8–45, 1996.

[80] G. Grätzer. *Lattice theory.* WH Freeman and Co, San Francisco, 1971.

[81] G. Grätzer. *Universal Algebra.* Springer, second edition, 1979.

[82] A. Hatcher. *Algebraic Topology.* Hatcher, December 2000.

[83] P. T. Johnstone. *Stone Spaces*. Cambridge University Press, August 1986.

[84] S. Lang. *Linear Algebra*. Springer, 3 edition, 1987.

[85] S. Lang. *Algebra*, volume 211. Graduate texts in mathematics, 2002.

[86] W. A. Luxemburg and A. C. Zaanen. *Riesz spaces*. North-Holland Publishing Company, 1971.

[87] J. Leech M. Kinyon and J. Pita Costa. Distributive skew lattices. *Submitted to Semigroup Forum*, 2013.

[88] S. Mac Lane. *Categories for the Working Mathematician*. Springer, 1998.

[89] L. Mirsky. A dual of dilworth's decomposition theorem. *American Mathematical Monthly*, 78(8):876–877, 1971.

[90] S. Oudot and D. Sheehy. Zigzag Zoology: Rips Zigzags for Homology Inference. In *Proceedings of the twenty-ninth annual symposium on Computational geometry*, pages 387–396, 2012.

[91] H. Edelsbrunner P. Bendich, S. Cabello. A point calculus for interlevel set homology. *Pattern Recognition Letters*, 33(11):1436–1444, 2012.

[92] A. Polishchuk and L. Positselski. *Quadratic Algebras, Clifford Algebras, and Arithmetic Witt Groups*. American Mathematical Society, 2005.

[93] P. Škraba and M. Vejdemo-Johansson. Parallel and scalable zig-zag persistent homology. In *NIPS 2012 Workshop on Algebraic Topology and Machine Learning.*, 2012.

[94] P. Škraba and M. Vejdemo-Johansson. Persistence modules: Algebra and algorithms. *arXiv*, cs.CG, February 2013.

[95] A. A. Tuganbaev. *Semidistributive Modules and Rings*. Mathematics and Its Applications. Springer, 1998.

[96] K. Yosida. On the representation of the vector lattice. *Proceedings of the Japan Academy, Series A, Mathematical Sciences*, 18(7):339–342, 1942.

[97] A. Zomorodian, G. Carlsson, A. Collins, and L. Guibas. Persistence Barcodes for Shapes. *International Journal of Shape Modeling (2oo5)*, pages 1–12, January 2013.

[98] A. J. Zomorodian. *Topology for computing*, volume 16. Cambridge University Press, 2005.